

POLITECNICO DI TORINO

Corso di Laurea in Ingegneria Aerospaziale



TESI DI LAUREA MAGISTRALE

Develop af a Sensorized Test Bench with Optical Fibers
for Electromechanical Drives Diagnostics

Supervisors

Prof. Paolo Maggiore
Ing. Matteo Dalla Vedova
Prof. Daniel Milanese
Prof. Davide Janner

Candidate

Denny Quadrini

March 2019

Contents

Abstract	V
Sommario	VII
Acknowledgements	VIII
1 Introduction	1
1.1 Objectives	1
1.2 Thesis Structure	2
2 Optical Fiber and Bragg Grating Principles	3
2.1 The Optical Fiber	3
2.2 The Bragg Grating	5
2.3 The Light Signal	6
3 Test Bench Design	7
3.1 Physical Support design	7
3.2 Source of Electric Power	13
3.3 Source of Thermic Power	13
3.4 Temperature Sensing and Control System	16
3.4.1 Introduction	16
3.4.2 Temperature Sensing System	19
3.4.3 Temperature Control System	22
3.4.4 Power Management System	26
3.4.5 Arduino UNO Electric Supply Power	28
3.4.6 Response to the Command Signal	28
3.5 Optical Signal Acquisition System	30
3.5.1 Introduction	30
3.5.2 FBG Interrogator	31
3.5.3 Optical Fiber	32
3.5.4 Acquisition Software	32
3.6 Test Bench Operation and Functional Block Diagram	34
4 Data Collection and Post-Processing	35
4.1 Introduction	35
4.2 Command Temperature Signal Setup	35
4.3 Sensed Temperature in the Isolated Volume	36

4.4	Optical Fiber and Pt-100 Sensor: Signal Comparison	38
4.4.1	Introduction	38
4.4.2	Useful Measurements	39
4.4.3	Interpolation	41
4.4.4	Sensed Temperature	42
5	Construction of a Temperature Sensor with Optical Fibers	43
5.1	Introduction	43
5.2	Acquisition and Data Handling Software	43
5.3	Conclusions	45
Appendix A: Develop of a Controller for a Servo Motorized Micrometer Head		46
	Introduction	46
	Components	47
	Functional Block Diagram	49
Appendix B: Develop of a Servo Motorized Micrometer Head		51
	Introduction	52
	Components	55
	Functional Block Diagram	61
Bibliography		61

List of Figures

2.1	Optical Fiber with Bragg Grating	3
2.2	Boundary Conditions between Core and Cladding	4
2.3	Broadband Signal Spectral Response	5
3.1	Anti-Vibration Table	8
3.2	Newport M-SG-22-2 Optical Breadboard	8
3.3	3D printed Adaptive Support for Peltier Module	9
3.4	Peltier Module inserted in the 3D Printed Adaptive Support	10
3.5	Physical Support System mounted on the Breadboard	11
3.6	Detail of the Physical Support System mounted on the Breadboard	12
3.7	Stabilized Power Supply	13
3.8	ET-031-08-15 Peltier module	14
3.9	Peltier Module Behavior at Hot Side Temperature 75 °C	15
3.10	Temperature Sensing and Control Functional Block Diagram	16
3.11	Functional Block Diagram of the PI Control	17
3.12	Signal PWM Modulation	18
3.13	Platinum Resistance Pt100 Detector with extended leads, 4 wire, thin film	19
3.14	Adafruit MAX31865 Platinum RTD-to-Digital Converter	20
3.15	Arduino UNO Board	22
3.16	IRF520 Power Mosfet	26
3.17	IRF520 Power Mosfet Characteristic at 25°C	27
3.18	Example of a Command Response	28
3.19	Command Test	29
3.20	Optical Signal Acquisition System	30
3.21	SmartScan FBG Interrogator	31
3.22	SmartScan FBG Interrogator Software Interface	33
3.23	Test Bench Functional Block Diagram	34
4.1	Command Temperature Signal	36
4.2	Sensed Temperature Signal, system well isolated	37
4.3	Sensed Temperature Signal, system badly isolated	37
4.4	Optical Signal Acquisition System	38
4.5	Optical Fiber VS Pt-100 Signals	39
4.6	Pt-100 Signal - Overshoot Peaks Isolation	40
4.7	Optical Fiber Signal - Overshoot Peaks Isolation	40
4.8	Data Interpolation	41
4.9	Optical Fiber VS Pt-100 Signals: Sensed Temperature	42

5.1	Acquisition and Data Handling Functional Block Diagram	45
5.2	Future Develop: Acquisition and Data Handling Functional Block Diagram	45
5.3	Tensioning of the Optical Fiber with the Servo Motorized Micrometer Head	46
5.4	SN754410 H-Bridge Simplified Schematic	48
5.5	SN754410 H-Bridge Pin Configuration and Functions	48
5.6	Data Acquisition and Position Control System - Servo Motorized Micrometer Head	49
5.7	Controller with related electronics and Servo Motorized Micrometer Head	50
5.8	Example of a Command Response of the Servo Motorized Micrometer Head	51
5.9	Servo Motorized Micrometer Head bending the spar	53
5.10	Servo Motorized Micrometer Head 3D CAD	53
5.11	Servo Motorized Micrometer Head	54
5.12	Faulhaber Epicycloidal Gearmotor with Adaptor for Micrometer Head	55
5.13	Faulhaber MCDC 2803 Motion Controller - Functional Block Diagram	57
5.14	Faulhaber MCDC 2803 Motion Controller - Pinout	57
5.15	Motion Controller and related electronics	58
5.16	Non-inverting Amplifier with a gain $G = 2$ - Dimentioning	59
5.17	LM 358 Dual Operational Amplifier - Pinout	59
5.18	Supply Power	60
5.19	Spar Bending System Functional Block Diagram	61
5.20	Response of the Optical Fiber with a 10 step command signal of 2 mm of tip displacement for each step	62

List of Tables

- 2.1 Typical Diameters of an Optical Fiber 4
- 3.1 Elements of the Anti-Vibration System 7
- 3.2 Newport M-SG-22-2 Breadboard Characteristics 7
- 3.3 Elements of the Physical Support System 12
- 3.4 TTi EL302RT Stabilized Power Supply Characteristics 13
- 3.5 Peltier Module Characteristics 15
- 3.6 Pt100 detector characteristics 19
- 3.7 Adafruit MAX31865 Main Features 21
- 3.8 Serial Communication Protocol 21
- 3.9 Arduino UNO Characteristics 23
- 3.10 Control Setting Parameters 24
- 3.11 Integer Gains 25
- 3.12 Absolute Maximum Ratings of the IRF520 Power Mosfet 27
- 3.13 SmartScan FBG Interrogator: Main Measurement and Processing Specifications 31
- 3.14 SmartScan FBG Interrogator: Mechanical, Environmental and Electrical Specifications 32
- 3.15 Fiber Specification 32
- 3.16 Grating Specification at 21 °C - Measurement Equipment: YOKOGAWA AQ637D 32
- 5.1 TMS-16 Servo Motorized Micrometer Head Characteristics 47
- 5.2 Serial Communication Protocol - MATLAB 50
- 5.3 Arduino Pinout 50
- 5.4 Faulhaber Series IE2-512 Precious Metals Brushed DC Motor with integrated Encoder - Main Characteristics 56
- 5.5 Faulhaber Series 23/1 Planetary Gearhead - Main Characteristics 56
- 5.6 Servo Motorized Micrometer Head Characteristics 56
- 5.7 Power Supply Main Characteristics 60

Abstract

This work focuses on how to measure a physical parameter using a special optical fiber as a transducer. The goal is to study a system that can be used to access to very small volumes where other sensors cannot because of their physical dimensions. Moreover, there are other advantages of using the optical fiber technology like the absence of electromagnetic interference and the very high sensibility and response speed of the sensor itself.

The optical fiber used in this work is like any other optical fiber used for example for digital high speed communication: the fiber is the medium through which the information propagates. The difference from the first ones is that it contains a Bragg grating, which is very small compared to the length of the fiber and acts like a punctual sensor.

It is possible to create more Bragg gratings within one optical fiber. This allows to measure different parameters and/or different points in a volume using only one channel of communication, reducing so the number of wires necessary to other technologies. Another advantage is that a Bragg grating is a passive sensor and it doesn't need to be supplied.

Sommario

Questo lavoro si concentra su come misurare un parametro fisico utilizzando una fibra ottica speciale come trasduttore. L'obiettivo è quello di studiare un sistema che può essere utilizzato per accedere a volumi molto piccoli dove altri sensori non possono a causa delle loro dimensioni fisiche. Inoltre, ci sono altri vantaggi nell'utilizzare la tecnologia delle fibre ottiche come l'assenza di interferenze elettromagnetiche e l'altissima sensibilità e velocità di risposta del sensore stesso.

La fibra ottica utilizzata in questo lavoro è come qualsiasi altra fibra ottica utilizzata ad esempio per la comunicazione digitale ad alta velocità: la fibra è il mezzo attraverso il quale si diffonde l'informazione. La differenza rispetto ai primi è che contiene un reticolo di Bragg, che è molto piccolo rispetto alla lunghezza della fibra e agisce come un sensore puntuale.

È possibile creare più reticoli di Bragg all'interno di una fibra ottica. Ciò consente di misurare diversi parametri e/o punti diversi in un volume utilizzando un solo canale di comunicazione, riducendo così il numero di fili necessari ad altre tecnologie. Un altro vantaggio è che un reticolo di Bragg è un sensore passivo e non deve essere alimentato.

Acknowledgements

Elogio e ringrazio i relatori per la disponibilità e la gentilezza. Mettono infatti volentieri a disposizione la loro competenza e sanno sempre dare le indicazioni giuste per la riuscita di qualsiasi progetto.

Ringrazio il futuro PhD Pier Calo Berri che mette a disposizione il suo cervello a tutti i ragazzi.

Ringrazio tutti i ragazzi del gruppo *Photonext* di quest'anno: Bruno Lavagnino, sempre presente e a disposizione in laboratorio con la sue competenze e la sua immancabile ironia; Alice Sgroi, che mi ha aiutato con le saldature; Guido Riva, che aiuta i ragazzi con le stampa 3D; Gioele Baima, Giuseppe Spampinato e Rachele Fausti, con cui abbiamo egregiamente lavorato insieme. Ringrazio Mauro Guerrera che mi ha aiutato a gestire il software dell'interrogatore ottico. Ringrazio tutti i ragazzi dell'istituto Boella per averci dato una mano a saldare i connettori delle fibre ottiche.

Ringrazio in generale tutti i ragazzi degli anni precedenti che ci hanno passato il testimone e tutti quelli che continueranno il nostro lavoro.

Ringrazio la mia famiglia che mi ha sostenuto in questi anni, in modo particolare mio padre. Grazie ai suoi sacrifici e al mio impegno sono riuscito a portare a termine questo percorso di studi.

Ringrazio la mia ragazza Beatrice che mi è stata vicino e gli amici più intimi che lo sono stati altrettanto, anche se in maniera differente ovviamente. Tra questi non posso non citare il mio coinquilino Giuliano Cammarata e il mio caro amico Francesco Viglione.

Ringrazio i compagni di merende e caffèini, con i quali mi vedo meno spesso, ma fa sempre piacere.

Infine, se mi sono dimenticato di qualcuno, portate pazienza. Tanto chi mi conosce bene lo sa che non ho una buona memoria.

Chapter 1

Introduction

In general, the optical fiber is used to send a signal for very long distances with very low signal loss. Its function is the same as a classical copper wire, apart from the performance reached in data transmission and in general the difference between the two type of technology. In the first case, when one would make a transducer, a circuit has to be designed. It means that the sensor has to be supplied with electric power and then the transduced information in terms of signal voltage is converted in the physical magnitude to be measured. With the optical technology it is possible to take advantage of the properties of the Bragg grating.

Sending a broadband signal within the fiber, there will be a reflection which is sent back to the source. Obviously, the input and reflected signals are not the same one. How will be explained later, the reflected signal intensity is maximum at a certain wavelength, and approximately zero far from that wavelength.

In some application there is the need to measure a certain magnitude with very high speed. These application could be for example the aerospace industry and those like this that involve the security and reliability of the systems, combined with the stringent technical requirements. Other applications could be somewhere one has to measure a physical parameter in a very small volume and there is no space to allocate a classic sensor and its related wires or where the environment could include electromagnetic interference related phenomena.

1.1 Objectives

The main objective of the work is to study how to build a very high speed temperature sensor using a *Fiber Bragg Grating* (FBG) as a transducer. To do so, usually one predicts the magnitude variation of the signal with some law. Some coefficient of the law is known, but others must be estimated. More difficult is to calculate how these coefficients vary in function of the parameter to be measured. This is particularly true for a temperature variation. It could be that these coefficients are known in the proximity of some standard reference magnitude. In this study was chosen to compare the signal of the optical fiber to a well-known signal got as a reference signal.

A traditional signal read from a resistive transducer, after the data processing, will generate a

temperature signal. These mechanism are known in the field of engineering and have been used and tested for a lot of applications. We expect that the optical fiber signal has to be analogue to the signal mentioned above. If the similarity between the two signal is captured, then is possible to transform the optical fiber signal in order to provide a temperature sensing. In this way, the magnitude signal of the wavelength reflected by the Bragg grating will be transformed in a temperature signal.

In the field of engineering we are more interested to what happens to a physical parameter like the instantaneous temperature in a certain point rather than to what really happens into the optical fiber.

1.2 Thesis Structure

In *Chapter 2* it will be described the optical fiber and Bragg grating principles. These are the two elements that allows the information to be transmitted through the fiber and to be modified if a variation of the external environment happens.

In *Chapter 3* it will be described how the test bench was built. First of all, a temperature system controller was made. It was used a thermic and vibration isolation system, in temperature controlled. In this chapter is explained also the system architecture and how the control is built, which components are used and why these components was chosen.

In *Chapter 4* it will be explained what type of command signal was chosen and why, how the data collection is set up, how was done the post-processing and what data were extrapolated. It will be explained how one can obtain a temperature signal from a wavelength signal. These considerations will allow to build a temperature sensor.

In *Chapter 5* it will be described how to build a temperature sensor using optical fibers. It will be described the used architecture. Moreover, it will be described the architecture of a real time data transmission system through an internet of things platform. This allows to share the data with different devices.

Chapter 2

Optical Fiber and Bragg Grating Principles

2.1 The Optical Fiber

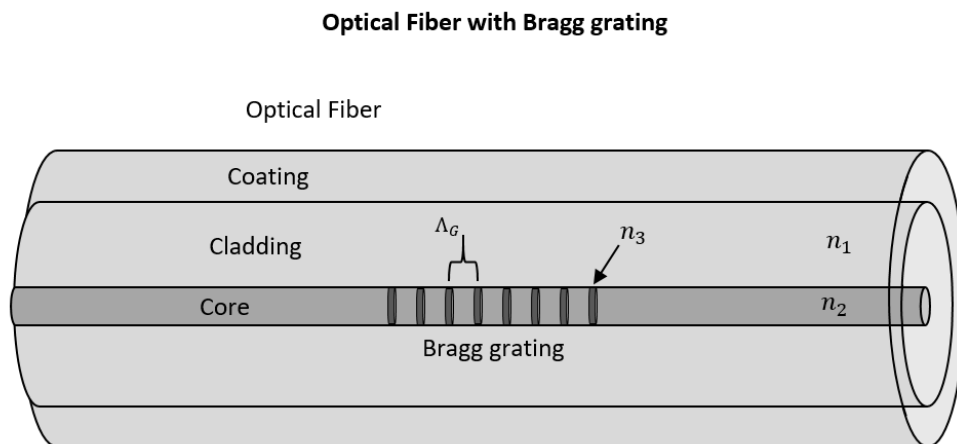


Figure 2.1: Optical Fiber with Bragg Grating

The optical fiber allows the signal to travel from the source to the Bragg grating and to be reflected to the power source. It is the medium through which the information propagates.

The optical fiber is made of a inner layer, the *core* and an outer layer, called *Cladding*. The cladding's aim is to focus the light signal into the core and allow it to follow the geometry of the wiring. This is why it has a lower refraction index. The outest layer, called *Coating*, is a safe protection layer and protects the optical fiber from the outer environment.

In the interface between the core and the cladding, the light ray follows the *Snell law*:

Typical diameters	[μm]
Core	8 - 60
Cladding	100 - 150
Coating	200 - 900

Table 2.1: Typical Diameters of an Optical Fiber

$$\sin(\theta_i) \cdot n_2 = \sin(\theta_r) \cdot n_1 \quad (2.1)$$

where:

- θ_i is the incidence angle
- θ_r is the refraction angle
- n_2 is the refraction coefficient of the core
- n_1 is the refraction coefficient of the cladding

Thus, it follows that:

$$\frac{\sin(\theta_r)}{\sin(\theta_i)} = \frac{n_2}{n_1} \quad (2.2)$$

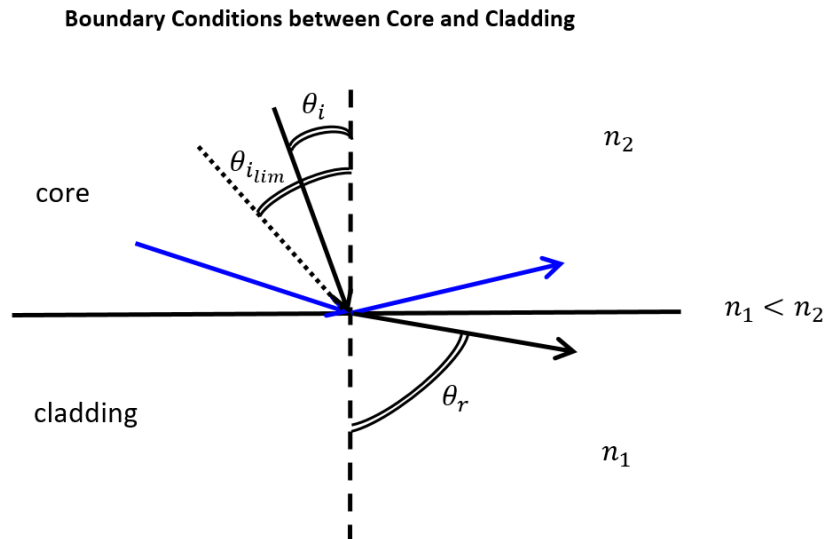


Figure 2.2: Boundary Conditions between Core and Cladding

From Figure 2.2 it can be seen what happens between the core and the cladding. If $n_1 < n_2$, then $\theta_r > \theta_i$ and the light ray will be focused near the core. This happens until the incidence angle is lower than the *limit angle*. When the incidence angle is equal to the limit angle, the refracted ray will propagate on the boundary between the core and cladding. The limit angle is the minimum incidence angle to be used for no signal loss. If the incidence angle is higher than the limit angle, the light ray will be simply reflected into the core. This case is colored blue in the figure.

2.2 The Bragg Grating

Normally, to manufacture the Bragg grating a germanium-doped silica fiber is used. This because this type of fiber is photosensitive, which means that the refractive index of the core changes with exposure to UV light. More recently, fiber Bragg gratings have also been written in polymer fibers. Using interference fringes from a sufficient power source, like an UV laser, it is possible to inscribe the grating on the core of the optical fiber.

When the incident broadband signal passes through the Bragg grating it is splitted in a reflected and transmitted components. There is one wavelength of the spectrum that is mainly reflected to the source. The Bragg grating therefore acts like a wavelength-specific reflector. It could be used also as an optical filter to cut certain wavelengths. The *Bragg wavelength* is the reflected wavelength of the spectrum which has the maximum relative intensity, compared to the incident spectrum. In figure 2.3 it can be seen how the input signal is modulated.

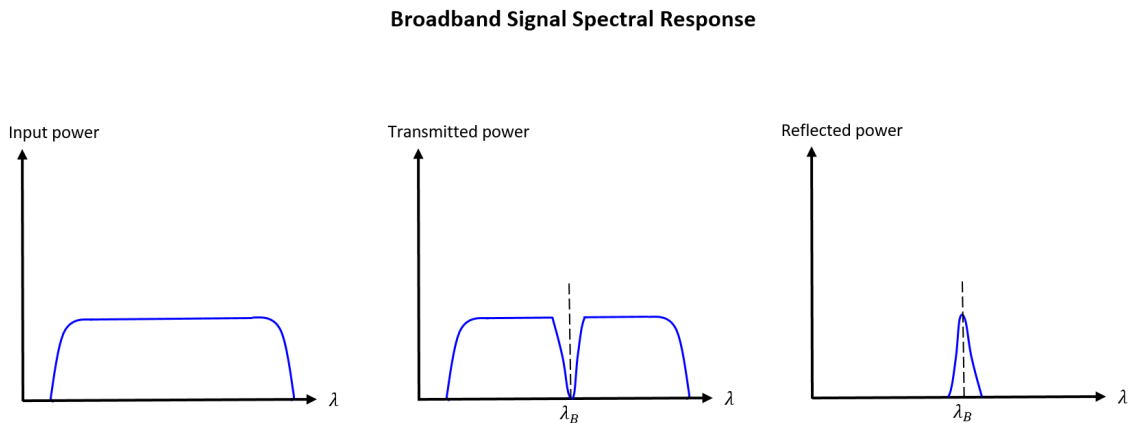


Figure 2.3: Broadband Signal Spectral Response

It follows the law:

$$\lambda_B = 2n_3\Lambda_G \tag{2.3}$$

where:

- λ_B is the Bragg wavelength
- n_3 is the refractive index of the grating
- Λ_G is the grating period

2.3 The Light Signal

When a Bragg grating is used like a sensor, the variation of the external environment or a load applied to the fiber causes an offset of the Bragg wavelength. This offset is due to the physical changes of the Bragg itself. So, considering the equation 2.3, a variation of the refractive index and/or a variation of the grating period happens.

Some study was present in the literature to explain how those variation take place. In particular, it's known that the variation of the Bragg wavelength can be described as:

$$\Delta\lambda_B = \lambda_B[(\alpha_f - \zeta_f)\Delta T + (1 - Pe)\Delta\epsilon] \quad (2.4)$$

where:

- α_f is the thermal expansion coefficient
- λ_B is the Bragg wavelength
- ζ_f is the termo-optic coefficient
- Pe is the photoelastic constant
- ΔT is the temperature variation, expressed in °C
- $\Delta\epsilon$ is the deformation variation, expressed in $\mu\epsilon = 10^{-6}\epsilon$

Taking into accounts the causes that involve the variation of the Bragg wavelength, now will be examined the case of a variation in temperature. To do so, the optical fiber must be installed loose to have no mechanical Bragg deformation.

The objective now is to consider a real signal, which evolves over time. In particular, a discretized signal. Although the response of the optical fiber moves at speed of light, when the information has to be collected, the response speed of the signal will depend from the sampling rate. The sampling rate is a characteristic of the instrument used to collect data. There is also the delay time related to the algorithm used to process the data and the machine where that algorithm runs. For a classic resistive sensor, additional delay time due to the time constant of the sensor itself has to be considered.

Chapter 3

Test Bench Design

3.1 Physical Support design

The physical support has the objective to create a temperature isolation system where the sensors will be allocated. Moreover, it must allocate the source of power. To avoid influence from the outer environment, a vibration isolation system must also be provided.

In the figure 3.1 it can be seen the anti vibration table used. It is made of a certain number of components which are reported in the table 3.1 below:

Number	Object
1	Support Structure
2	Air Tanks
3	Air Dumpers
4	Anti Vibration Granite Table
5	Breadboard

Table 3.1: Elements of the Anti-Vibration System

To fit the isolated system to the anti-vibration table, a breadboard is used. The available one is reported in figure 3.2. In the table 3.2 below are reported instead the breadboard characteristics:

Parameter	Description
Width	600 mm
Length	600 mm
Thikness	59 mm
Mounting Holes	M6
Holes Pitch	25 mm

Table 3.2: Newport M-SG-22-2 Breadboard Characteristics

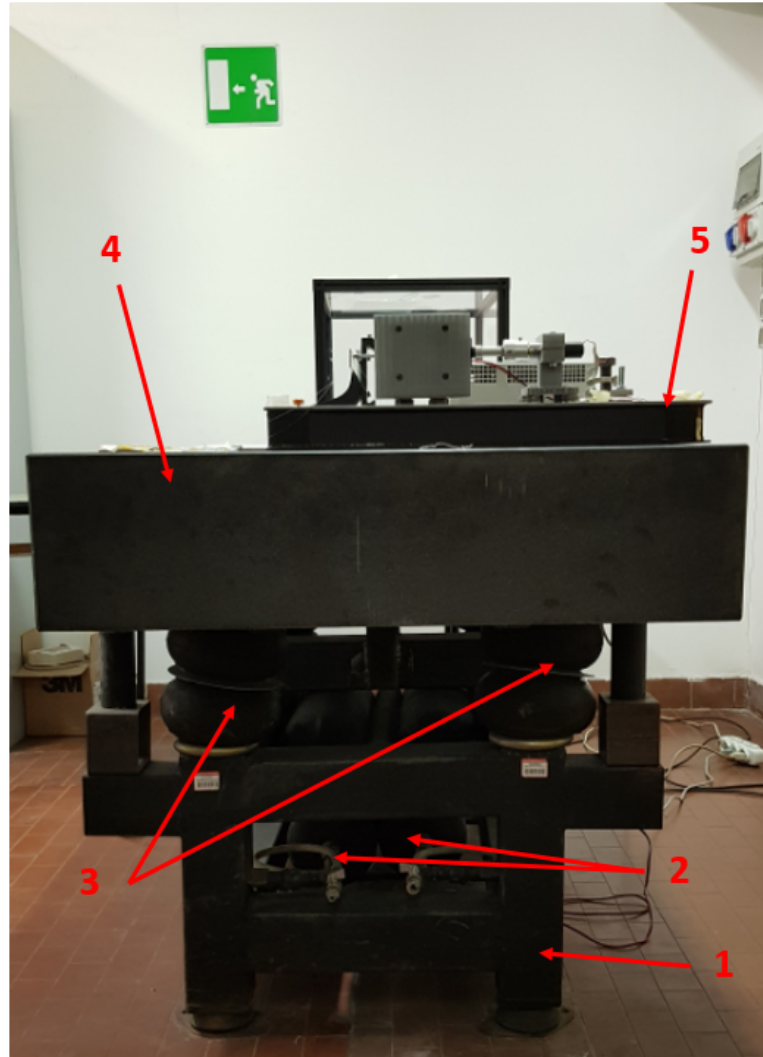


Figure 3.1: Anti-Vibration Table



Figure 3.2: Newport M-SG-22-2 Optical Breadboard

Now there is the need to find a system to connect the Peltier module and the various sensors to the anti-vibration system. Since in the Peltier cell the heat is transferred from the cold side to the hot side through the thickness, no theoretically heat is transferred through the sides. So, a 3D printed plate can be used to accommodate the Peltier cell and allow it to be fixed to the structure. In the figure 3.3 can be seen the two configuration taken into consideration. Finally, the chosen plate can be seen in the figure 3.4.

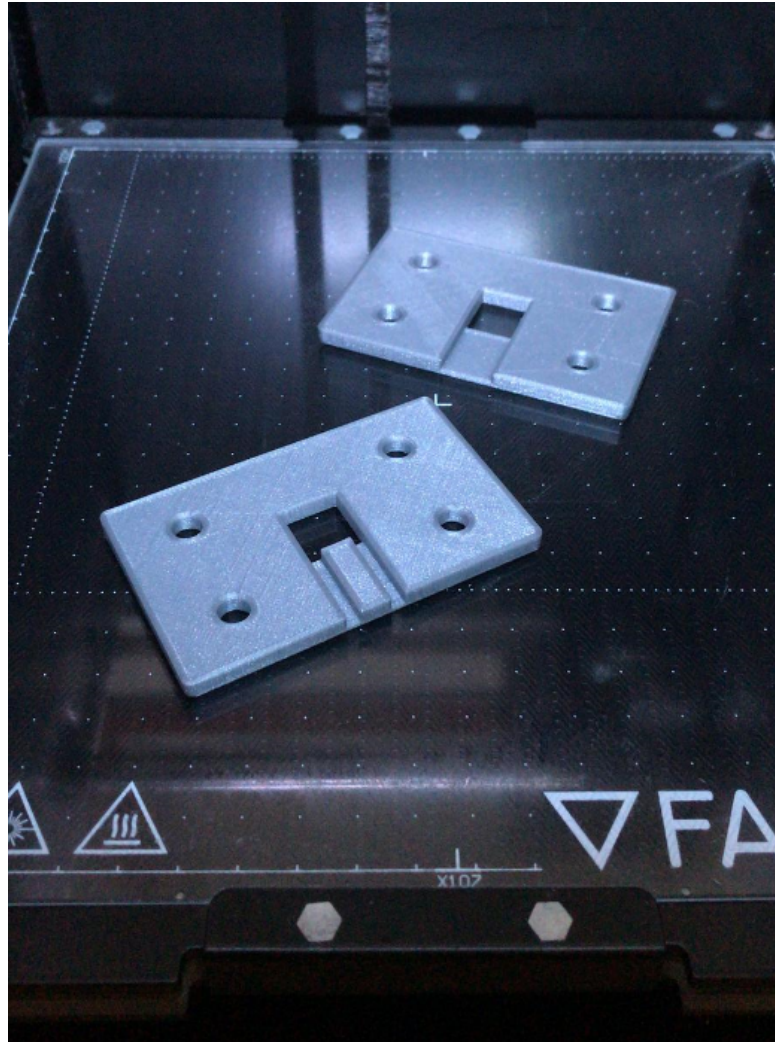


Figure 3.3: 3D printed Adaptive Support for Peltier Module

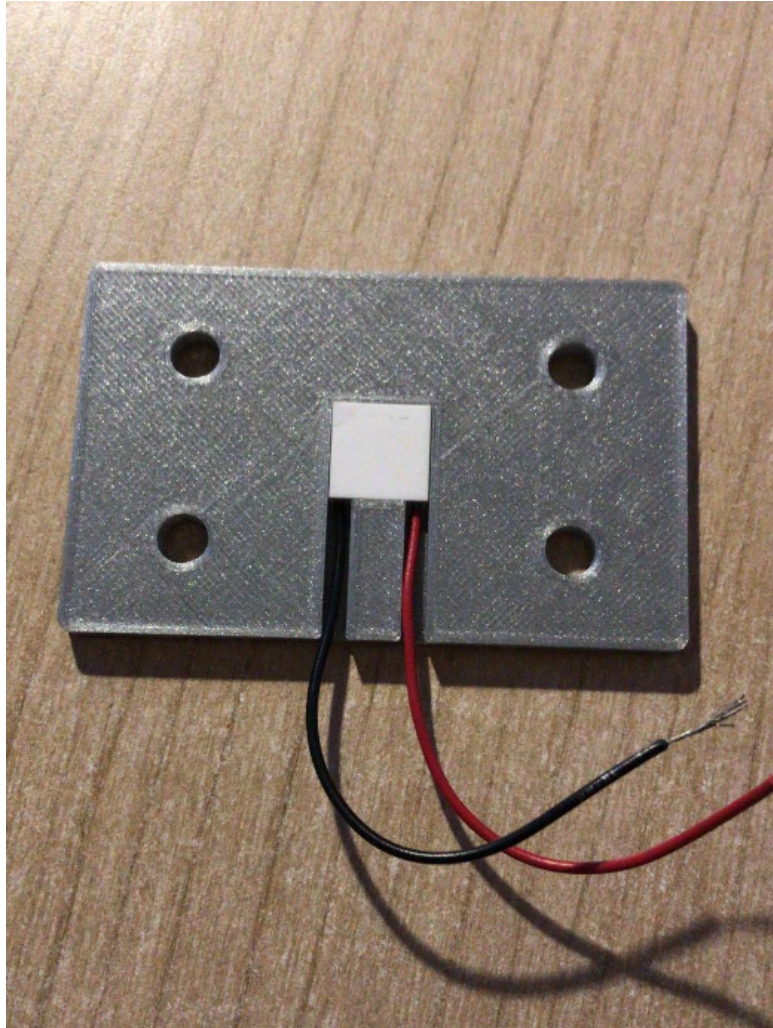


Figure 3.4: Peltier Module inserted in the 3D Printed Adaptive Support

In the same figure one can observe that the support shape allows to the Peltier cell wires to exit out from one side. The Pt-100 sensor and the optical fiber are instead inserted in the other side. This is the best choice in order to optimize the available space and in order to avoid electromagnetic interactions between the power cables and the signal cables.

The other components needed to complete the isolation system are two aluminium plates, a silicone gasket, a pressor and the mechanical connections to keep all the components together and fixed to the breadboard.

In the figure 3.5 it can be seen the physical support system mounted on the breadboard.

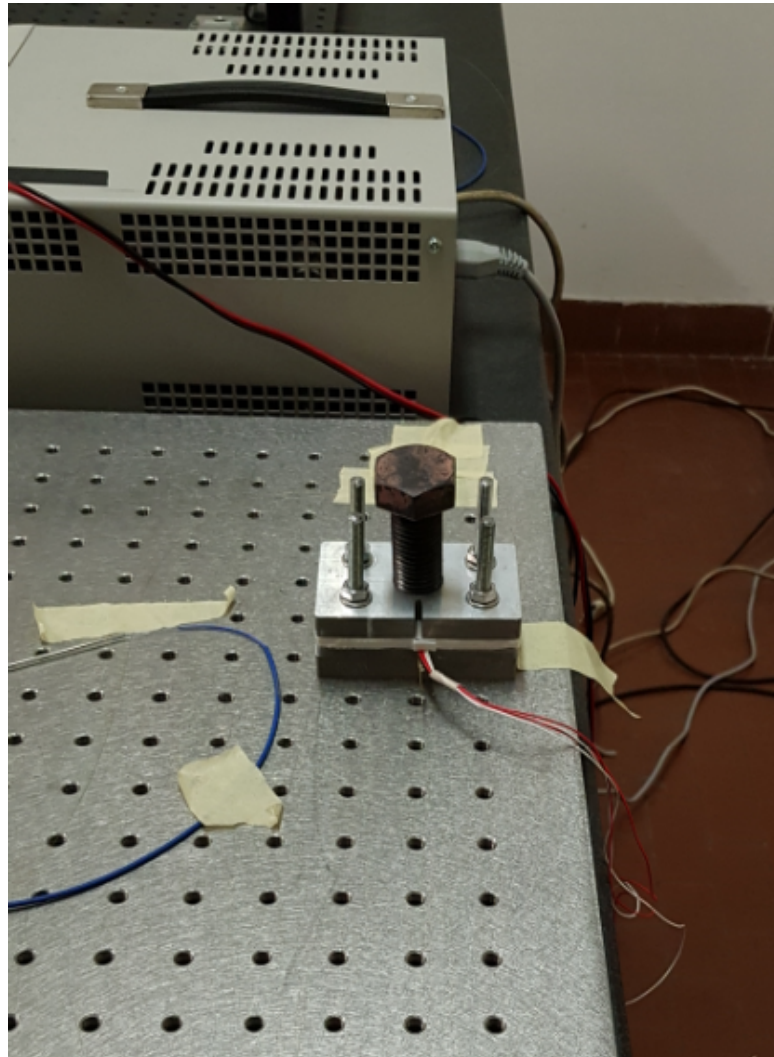


Figure 3.5: Physical Support System mounted on the Breadboard

In the figure 3.6 it can be seen a detail of the physical support. The various elements of the physical support are instead reported in table 3.3:

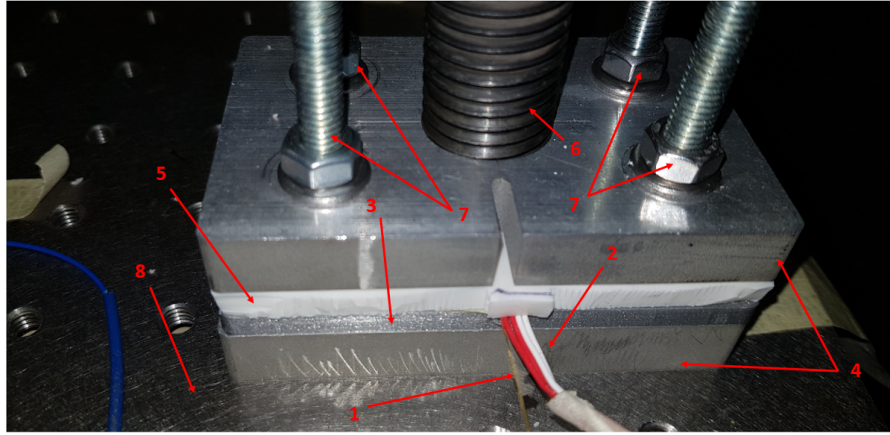


Figure 3.6: Detail of the Physical Support System mounted on the Breadboard

Number	Object
1	Optical Fibre
2	Pt-100 Sensor Wires
3	3D Printed Support
4	Aluminium Plates
5	Silicone Gasket
6	Pressor
7	Mechanical Connections
8	Optical Breadboard

Table 3.3: Elements of the Physical Support System

3.2 Source of Electric Power

The source of electric power available in the laboratory is the power supply reported in figure 3.7. In the table 3.4 below are instead reported the characteristics of the two channels available:



Figure 3.7: Stabilized Power Supply

Characteristic	Channel 1	Channel 2
Max Output Current [A]	2	2
Max Output Voltage [V]	60	30

Table 3.4: TTI EL302RT Stabilized Power Supply Characteristics

3.3 Source of Thermic Power

The source of thermic power has the objective to vary the temperature of the system. The source of thermic power chosen in this experiment is a *Peltier cell*. The system can be considered as a plane source of power. The Peltier cells works with the *thermoelectric effect*, which is the direct conversion of temperature differences to electric voltage and vice versa via a thermocouple.

A thermoelectric device creates voltage when there is a different temperature on each side. Conversely, when a voltage is applied to it, heat is transferred from one side to the other, creating a temperature difference. At the atomic scale, an applied temperature gradient causes charge carriers in the material to diffuse from the hot side to the cold side. This effect causes the Peltier cell to behave like a heat pump that absorbs heat on the cold side and gives it over the hot side.

The thermoelectric effect can be used to generate electricity, measure temperature or change the temperature of objects. Because the direction of heating and cooling is determined by the polarity of the applied voltage, thermoelectric devices can be used as temperature controllers. In the most application the Peltier cell is used as a cooler, since that if one would to build a heater, a resistor can be used too. The main difference is that in the last case, the heat transfer is a thermodynamically irreversible process. In figure 3.8 below the chosen Peltier cell can be seen.

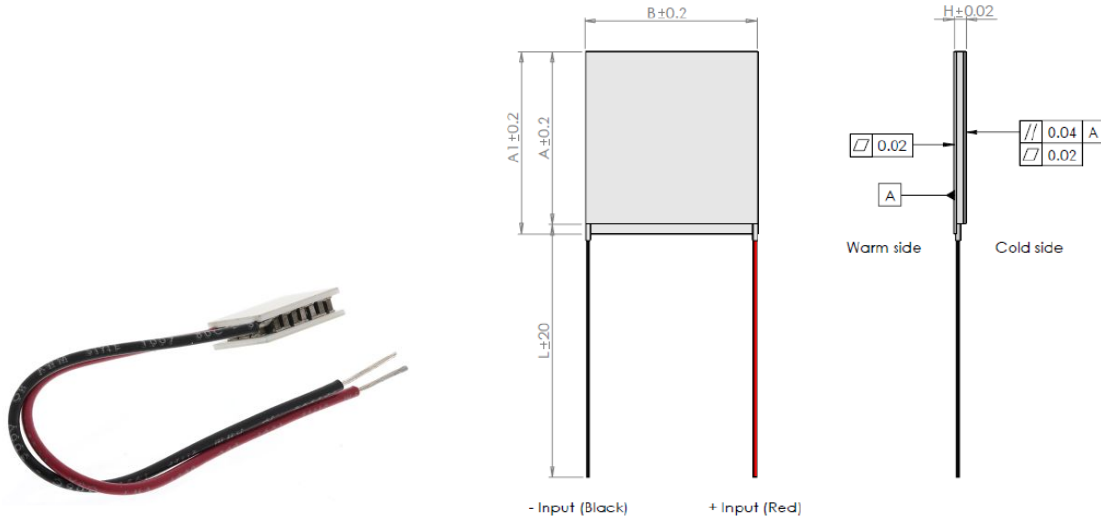


Figure 3.8: ET-031-08-15 Peltier module

The choice was done considering the following aspects:

- Physical dimensions of the Peltier
- Maximum output current of the electric power supply
- Peltier supply voltage
- Peltier maximum absorbed current

In table 3.5 above are reported the chosen Peltier module characteristics. There are reported the electric and dimentional characteristics.

$P_{C_{max}}$ is defined as the cooling power when $\Delta T = 0$ and $I = I_{max}$. Other parameters are reported in the data sheet, like the Peltier behavior in function of its hot side temperature. In figure 3.9 it is possible to see an example of these parameters at hot side temperature 75 °C.

The COP is the *coefficient of performance* and is defined as the heat absorbed at the cold side divided by the input power of the Peltier element. There is then a current value that maximize the removed heat from a system. This parameter is useful when a cooler system has to be designed. In this case, in general, the waste heat is more than the removed heat.

In our case, we do not need to cool the system but to provide heat and rise the temperature

Parameter	Value	Unit
I_{max}	2.2	A
V_{max}	3.8	V_{dc}
$P_{C_{max}}$	5.3	W
ΔT_{max}	74	$^{\circ}C$
A	13	mm
$A1$	13	mm
B	13	mm
H	3.8	mm
L	100	mm

Table 3.5: Peltier Module Characteristics

from the ambient temperature until a certain sufficient high value of temperature. The maximum temperature reached must be lower than $90^{\circ}C$ for the best long term performance of the Peltier module.

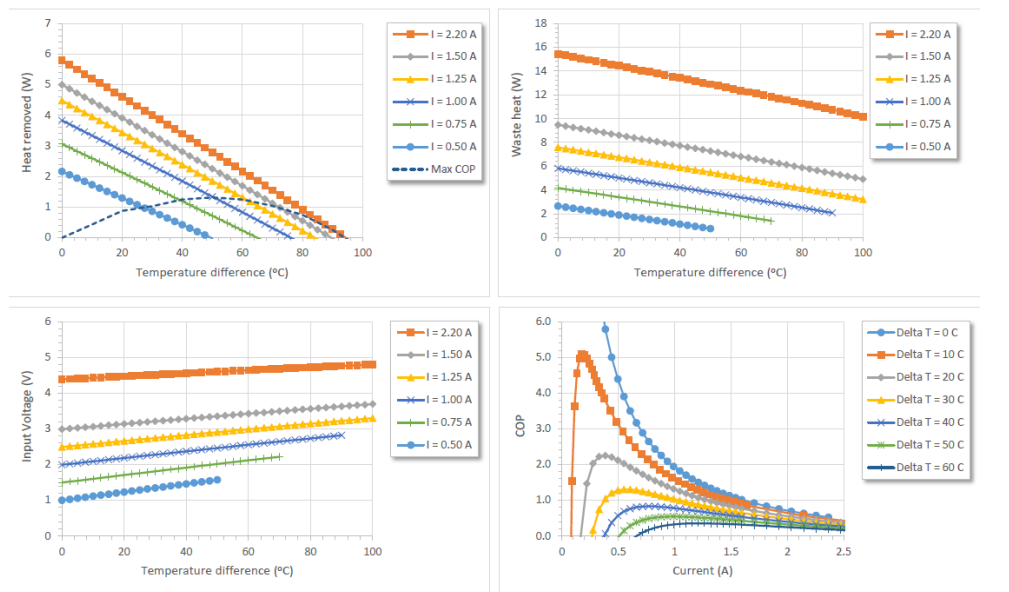


Figure 3.9: Peltier Module Behavior at Hot Side Temperature $75^{\circ}C$

3.4 Temperature Sensing and Control System

3.4.1 Introduction

The temperature sensing and control system has the objective to sense the temperature of the system in order to control the temperature of the system itself. The sensed temperature signal is used like a feedback signal to compare with the command temperature signal. The error between the command temperature and sensed temperature will be used to control the Peltier module. Looking the functional block diagram reported in figure 3.10 below, it is possible to describe how this process works.

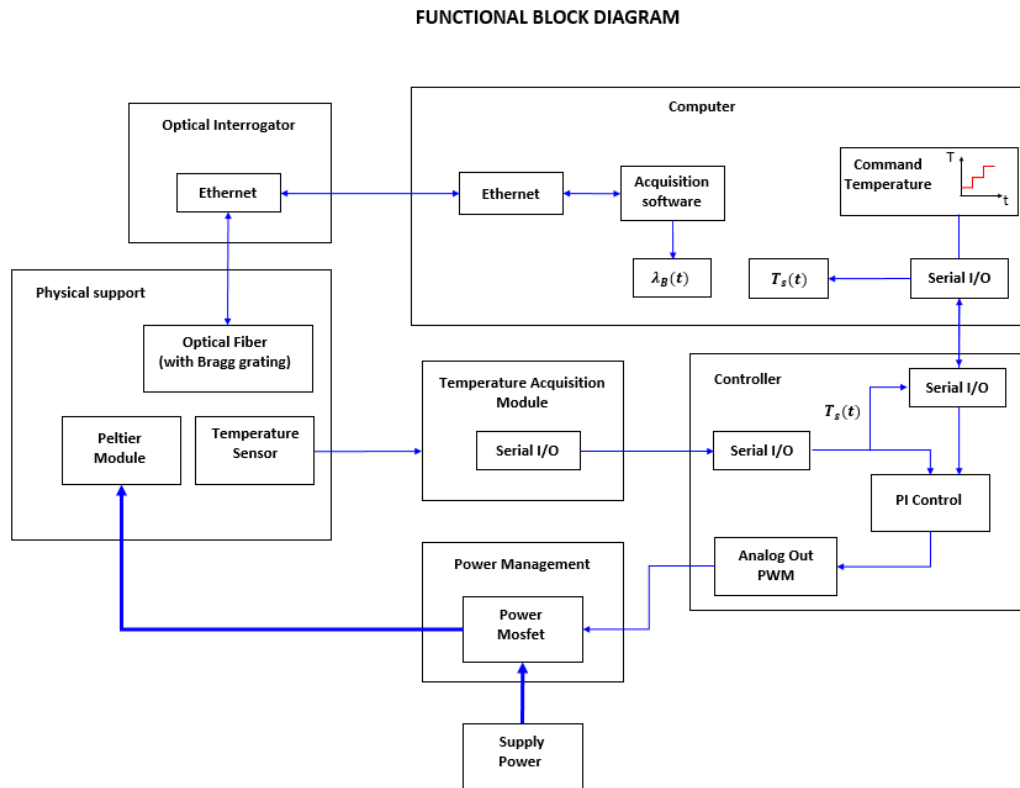


Figure 3.10: Temperature Sensing and Control Functional Block Diagram

In the isolated volume inside the physical support, a temperature variation causes a variation of the resistor resistance. The resistance will not be measured directly, but by measuring the voltage at the ends of the resistor with the well-known Ohm law. When the voltage variation is measured with a certain sample rate while time changes, it will be obtained a voltage signal whose module is proportional to the temperature module. The voltage signal is then transformed into a temperature signal which is provided to the controller via a serial bus. This function is carried out by the temperature acquisition module.

When the sensed temperature signal is obtained by the controller, it is compared with the command temperature signal. The error in a certain time and the error integral are used then to compute and provide a voltage signal to the power management system. The voltage signal is computed with a *Proportional Integrative Control*. The block diagram of the PI controller is shown in figure 3.11 below and where:

- T_C is the Command Temperature
- T_S is the Sensed Temperature
- e is the error measured between the command and the sensed temperature
- K_p is the Proportional Gain
- K_0 is the Bias
- K_i is the Integral Gain
- V_p is the Proportional Voltage
- V_i is the Integral Voltage
- V is the Voltage to be sent to the power management system

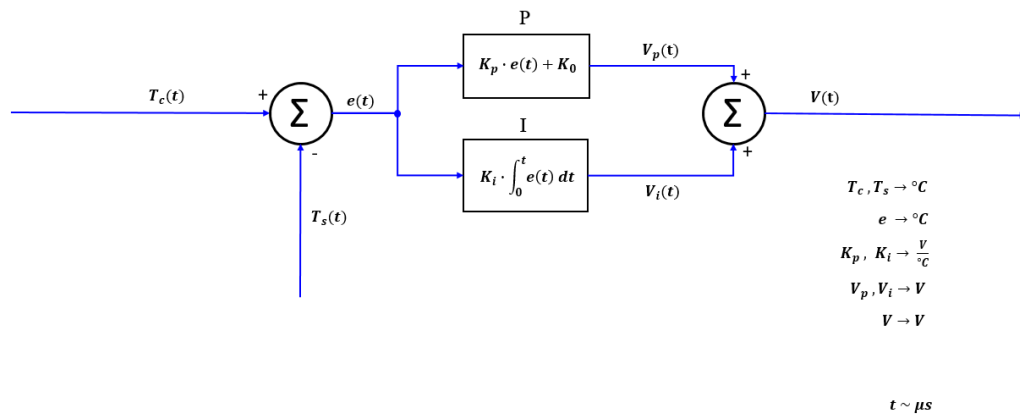


Figure 3.11: Functional Block Diagram of the PI Control

Once the algorithm has been implemented, the most difficult thing is to set the K_p , K_0 and K_i values in order to have the best response performance of the system. Usually this values are set experimentally or following those configurations which best fits in some application, normally referenced in literature.

In a control loop, the controller *Bias* is a constant amount added to or subtracted from the action that a controller would normally take with a particular gain. The bias provide to rise a little the commanded temperature. This is useful since the Peltier module is not continually power supplied. Thus, one band of operation is defined. When the commanded temperature is reached, the control will not command any voltage to the power management system so the sensed temperature start decreasing. In this way the desired temperature always stays in the band of operation, which is between the temperature of a new control loop and the commanded temperature.

The integrative control loop is saturated to avoid overflow, since a certain number of bit can be used to memorize a maximum finite integer value which is 2 elevated to the number of bits used to store the information minus one.

Once the voltage has been calculated, the controller writes on the analogic output via a *Pulse Width Modulation*. This type of modulation is used in many digital devices. Since a digital value of voltage can be high or low, to create a signal whose module is between the two extreme values, an over-time modulation of the signal is done. In the figure 3.12 below it can be seen a *PWM* modulation.

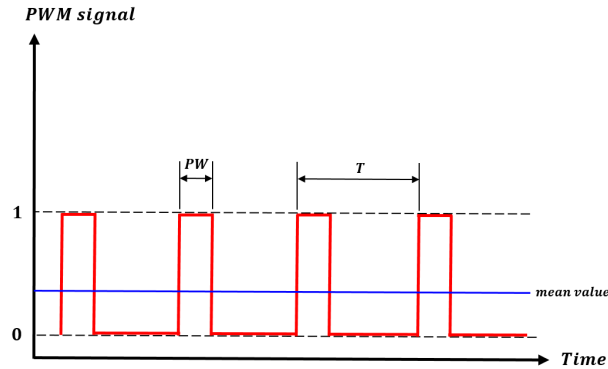


Figure 3.12: Signal PWM Modulation

The mean value to be provided to the analog output is related to the *Duty Cycle*:

$$D = \frac{PW}{T} \cdot 100\% \quad (3.1)$$

where:

- D is the duty cycle
- PW is the pulse width, that is the active time of the pulse in the signal period
- T is the total period of the signal

For example, if at the 1 logic level corresponds a voltage of 5V, then if one want to obtain a voltage of 2.5V, the duty cycle must be 50 %. This law is particularly simple in case of square wave, because the rms voltage value is equal to the mean value.

Looking to the figure 3.10, once the correct voltage has been provided to the power management system, this one have to transform the voltage signal into a current signal, since the Peltier module is commanded in current at a certain fixed value of voltage. The power management system must then convert a low power signal into a power signal.

Once the Peltier module is commanded, a temperature variation on the isolated volume occurs. The temperature sensor acquires a new value and the cycle restarts from the beginning.

Since the controller alone is able to maintain only a certain temperature, the command temperature signal is given externally, using *MATLAB*[®] to generate the commanded temperatures at the given times. This information is then sent from the computer to the controller through the USB serial bus. In this way, the commanded temperature signal is very reliable because of it is synchronized with the computer clock. Moreover, the information about the sensed temperature can be sent back to the computer and the same *MATLAB*[®] could be used to plot what happens.

3.4.2 Temperature Sensing System

As a temperature sensor, it was chosen a Pt100. This is a resistive sensor, which means that its resistance vary in function of the temperature. It is called Pt-100 because it is a Platinum resistor whose resistance is 100 Ω when the sensed temperature is 0 $^{\circ}\text{C}$.

In the table below it can be found the sensor characteristics:



Figure 3.13: Platinum Resistance Pt100 Detector with extended leads, 4 wire, thin film

Parameter/Object	Value/Description
Sensor Type:	Pt100 (100 Ω @ 0 $^{\circ}\text{C}$)
Construction:	Thin film, 10 mm tails
Temperature Range:	-50 $^{\circ}\text{C}$ to 250 $^{\circ}\text{C}$
Ice Point Resistance:	100 Ω
Fundamental Interval (0-100 $^{\circ}\text{C}$):	38.5 Ω (nominal)
Self-Heating:	< 0.5 $^{\circ}\text{C}/\text{mW}$
Thermal Response:	0.1s
Stability:	$\pm 0.05\%$

Table 3.6: Pt100 detector characteristics

How it can be seen from figure 3.13, this sensor has four wires with the same length, two connected to one sensor end and two to the other end. This configuration allows to compensate the wires resistance and to measure only the sensor resistance. To measure the voltage value at the sensor ends and then measure its resistance using the Ohm law, two circuits with a Wheatstone bridges has to be made. A reference resistor is used to make the bridges. Moreover, this circuit must contain operational amplifier with gains optimized to allow to measure the voltage at the sensor ends with a very low current. This because an exceed current can rise the sensor temperature via the *Joule Effect* and alter consequently the measure.

To fulfill this task was chosen an integrated circuit which works as temperature acquisition module. It can be seen in the figure 3.14 below:

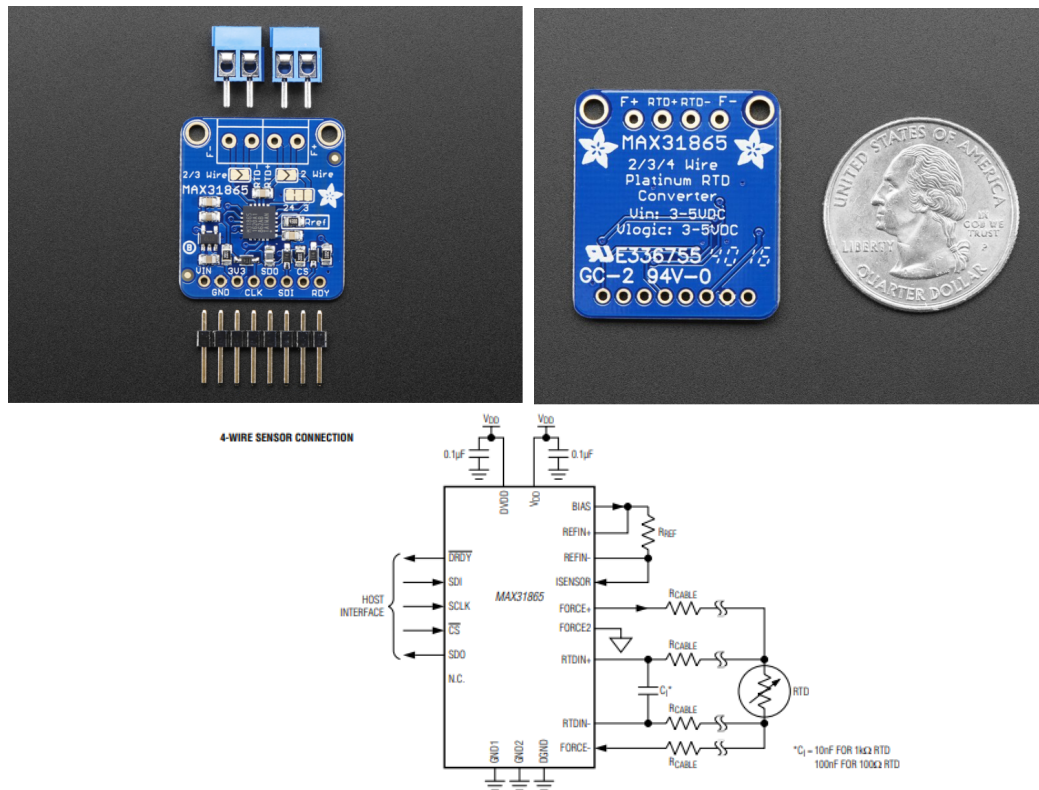


Figure 3.14: Adafruit MAX31865 Platinum RTD-to-Digital Converter

On the top of the module it can be seen the connections for the Pt-100 sensor; on the bottom there are the supply connections and the pins for serial communication with an external device. The reference resistor for a Pt-100 sensor is 430 Ω . An operating scheme of the integrated circuit can be seen in figure 3.14, on the bottom.

In the table below are reported instead the main features of the integrated circuit:

This module converts directly the resistance of the Pt-100 sensor in a digital value of temperature, expressed in $^{\circ}\text{C}$. Looking to the figure 3.10, if one want to estimate the *Delay Time* of the sensing temperature system, this is the sum of the delay time due to the thermal response of the sensor, the time taken by the acquisition module to convert the analogue value of the

Parameter	Value/Description
Resolution:	15 bit ADC
Nominal Temperature Resolution:	0.03125 °C
Total Accuracy:	0.5 °C max (All Operating Conditions)
V_{REF} Inputs:	Fully Differential
Conversion Time:	21 ms
Input Protection:	± 45 V

Table 3.7: Adafruit MAX31865 Main Features

resistance to the digital value of temperature and the time taken by the communication system to provide the data to the controller. So, the delay time has got the following expression:

$$t_d = t_s + t_m + t_c \quad (3.2)$$

where:

- t_d is the Delay Time
- t_s is the Delay Time due to the Thermal Response of the Sensor
- t_m is the Delay Time due to the Analogic-to-Digital Conversion
- t_c is the Delay Time due to the serial communication

The delay time tells how much time passes for a real time value of temperature before it can be used by the controller in a feedback loop. Looking to the table 3.13 and table 3.7, t_s and t_m are declared in the data sheets published by the constructors. Some consideration must be done to estimate t_c , because it depends on the serial communication protocol used between the temperature acquisition module and the controller. In the table below, it is possible to see the communication protocol characteristics:

Parameter	Value
Start Bit	1
Data Bits	8
Parity Bits	0
Stop Bits	1
Baud Rate	115200 bit/s

Table 3.8: Serial Communication Protocol

Handling those information, the Delay Time due to communication can be estimated as follow:

$$t_c = \frac{TotalBits}{BaudRate} = \frac{10}{115200} = 8.681 \cdot 10^{-5} s = 0.087 ms \quad (3.3)$$

How expected, this value is the lowest one and it is a second order term. However, it is possible to lower this term using a synchronous communication protocol, rising so one order of magnitude the baud rate or using a more performant controller. Two controllers also can be used, one for the temperature control loop and one used for data transmission. This because the controller used in this case has only one processor.

Taking into account the considerations above, the Delay Time can be written as:

$$t_d = 100 + 21 + 0.087 = 121.087 ms \quad (3.4)$$

If one would to plot the data, additional time to communicate with the computer is needed. Moreover, there is the possibility that the control works at a lower speed than the temperature sensing system. This can depend from some external factors, like the load to be controlled. In this case, the most limitations depend on the Peltier cell: the control must not allow the smelting of the welding between the two faces of the cell.

3.4.3 Temperature Control System

The Controller used in this work is the Arduino UNO. In figure 3.15 below it is showed the controller:



Figure 3.15: Arduino UNO Board

The Arduino is an open space platform very famous in the maker field. The platform allows to program the microcontrollers with a procedural language which is similar to the C language. The Arduino Uno instead is a very cheap electronic device whose technology is based on the microprocessor mentioned above, and provide also input and output interface with external

devices. It is good when the required performance is not very high. The Arduino UNO is the most used, robust and documented board of the whole Arduino family.

The Arduino Uno characteristics are shown in the table 3.9.

Parameter/Object	Value/Description
Microcontroller:	ATmega328P
Operating Voltage:	5V
Input Voltage (recommended):	7-12V
Input Voltage (limit):	6-20V
Digital I/O Pins:	14
PWM Digital I/O Pins:	6
PWM Output bits:	8
Analog Input Pins:	6
DC Current per I/O Pin:	20 mA
DC Current for 3.3V Pin:	50 mA
Flash Memory:	32 KB (0.5 KB used by bootloader)
SRAM:	2 KB
EEPROM:	1 KB
Clock Speed:	16 MHz
LED BUILTIN:	13
Length:	68.6 mm
Width:	53.4 mm
Weight:	25 g

Table 3.9: Arduino UNO Characteristics

As mentioned above and looking at the figure 3.10, the main objective of the controller is to control the temperature in the isolated volume and to communicate with the external devices. Those ones are the temperature acquisition module, from which the controller receives the actual temperature signal and the computer, from which the controller receives the command temperature signal. Moreover, the controller must be able to send the sensed temperature signal back to the computer, so that this parameter could be plotted. To communicate with the computer and with the temperature acquisition module is used a serial communication protocol.

The parameters of the communication protocol between the controller and the temperature acquisition module was described in table 3.8. These are the same parameters used in the communication protocol between the controlled and the computer (MATLAB[®]).

In telecommunication and data transmission, serial communication is the process of sending data one bit at a time, sequentially, over a communication channel or computer bus. This is in contrast to parallel communication, where several bits are sent as a whole, on a link with several parallel channels.

Arduino Uno has a number of facilities for communicating with a computer, another Arduino board, or other microcontrollers. The ATmega328 provides UART TTL (5V) serial communication, which is available on digital pins 0 (RX) and 1 (TX). An ATmega16U2 on the board

channels this serial communication over USB and appears as a virtual com port to software on the computer. The 16U2 firmware uses the standard USB COM drivers, and no external driver is needed. However, on Windows, a .inf file is required. The Arduino Software (IDE) includes a serial monitor which allows simple textual data to be sent to and from the board. The RX and TX LEDs on the board will flash when data is being transmitted via the USB-to-serial chip and USB connection to the computer (but not for serial communication on pins 0 and 1).

A SoftwareSerial library allows serial communication on any of the Uno’s digital pins. The ATmega328 also supports I2C (TWI) and SPI communication. The Arduino Software (IDE) includes a Wire library to simplify use of the I2C bus; see the documentation for details. For SPI communication, use the SPI library.

Looking to the figure 3.10 and considering that the control loop acts after a certain time to avoid the Peltier Cell to damage, it follows that the most important parameters of the control are the *Control Loop Delay Time* and the various gains of the PI Control.

A good response of the system was obtained experimentally considering the following parameters reported in table 3.10.

Parameter	Value	Unit
K_p	1.2745	$\frac{V}{^\circ C}$
K_0	1.2549	V
K_i	0.1176	$\frac{V}{^\circ C_s}$
Loop Control Delay Time:	250	ms

Table 3.10: Control Setting Parameters

The gains parameters in table 3.10 were obtained from integer values. However, some consideration has to be done to explain where these results come from.

Before doing that, a consideration of the following factors that affects the table 3.10 parameters have to be done. These factors are the:

- Max operating voltage of Arduino Uno (also provided to the digital PWM outputs), V_{max}
- Numbers of bits dedicated to the digital PWM output, n_{Bits}
- System operating conditions

The *Loop Control Delay Time* is the parameter which is more affected by the system operating conditions. This because if the control acts at very high speed and so at very low loop control delay time, this could overload the Peltier module. What happens is that the soldering between the Peltier cell’s plates suffers the smelting phenomena due to the high temperature reached, so damaging itself.

If instead the loop control delay time is set to very high values, this results in a too low control speed and the control becomes ineffective and fails to be particularly reactive to the temperature changes required by the command signal.

The gain values were set in order to guarantee the best dynamic performance of the system. The integer values of setted gains are reported in the table below:

Parameter	Value	Unit
k_p	65	$\frac{1}{^\circ C}$
k_0	64	-
k_i	6	$\frac{1}{^\circ C s}$

Table 3.11: Integer Gains

The digital PWM output can be handled by a function that accepts integer values as argument. Obviously, the zero value is the minimum, since this corresponds to no voltage to the output. With n_{Bits} dedicated to the PMW output, the *Maximum Integer Value Storable* is:

$$value_{max} = 2^{n_{Bits}} - 1 \quad (3.5)$$

Which means that in this case:

$$value_{max} = 2^8 - 1 = 255 \quad (3.6)$$

If one writes this value, the duty cycle will corresponds to 100%, and in this case the provided voltage to the PWM output will be 5V.

This means also that the *Voltage Signal Resolution* will be:

$$Res = \frac{5}{255} = 19.6 \text{ mV} \quad (3.7)$$

Now, the gains value reported in table 3.10 can be computed as follow:

$$K_p = k_p \cdot \frac{V_{max}}{n_{Bits}} = 1.2745 \frac{V}{^\circ C} \quad (3.8)$$

$$K_0 = k_0 \cdot \frac{V_{max}}{n_{Bits}} = 1.2549 \text{ V} \quad (3.9)$$

$$K_i = k_i \cdot \frac{V_{max}}{n_{Bits}} = 0.1176 \frac{V}{^{\circ}C_s} \quad (3.10)$$

3.4.4 Power Management System

Since the Peltier module is commanded in current and at maximum voltage, some device to transform the voltage signal of the controller into a power signal to be provided to the Peltier Cell is needed. Usually for this purpose a power mosfet is used. The selected one can be seen in figure 3.16

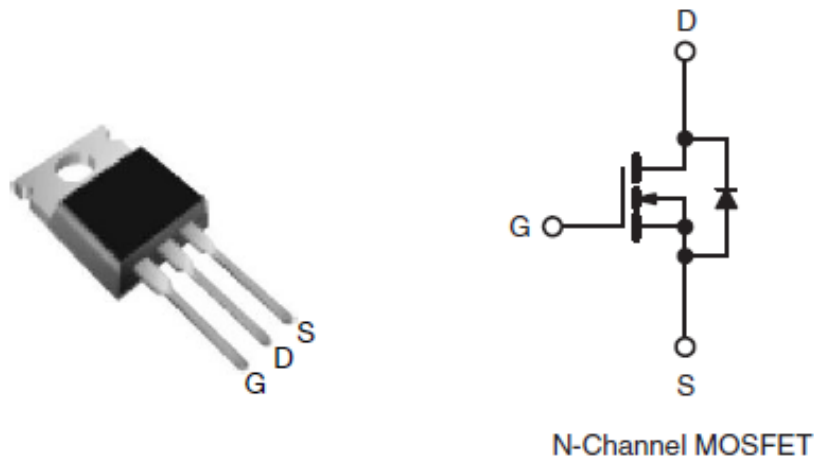


Figure 3.16: IRF520 Power Mosfet

In the table below are reported instead the absolute maximum ratings of the power mosfet:

Looking to the table 3.12, it is possible to explain why this mosfet has been selected. The *Drain-Source Voltage* to provide to the Peltier cell is lower than the maximum admitted, and it's equal to the maximum voltage to be supplied to the Peltier module (3.8 V). The *Gate-Source Voltage* is the voltage provided by Arduino (5 V), and is lower than the maximum admitted. Finally, the maximum continuous *Drain Current* is higher than the maximum current that could be absorbed by the Peltier Cell (2.2 A). This is also a conservative hypothesis because if the current is pulsed into the power mosfet, the maximum admitted value rises up until 37 A.

Moreover, if one looks to the figure 3.17, referring to the parameters V_{DS} and V_{GS} above, it can be seen that with these conditions the IRF520 saturates the current at 2 A. This is good in order to save the Peltier Cell from overcurrent. Finally, it can be observed in the same figure that the in current response characteristic is linear until about 1 V.

Parameter	Symbol	Limit	Unit
Drain-Source Voltage	V_{DS}	100	V
Gate-Source Voltage	V_{GS}	± 20	V
Continuous Drain Current ($V_{GS} = 10$ V, $T_C = 25$ °C)	I_D	9.2	A
Continuous Drain Current ($V_{GS} = 10$ V, $T_C = 100$ °C)	I_D	6.5	A
Pulsed Drain Current	I_{DM}	37	A
Linear Derating Factor		0.40	W/°C
Single Pulse Avalanche Energy	E_{AS}	200	mJ
Repetitive Avalanche Currenta	I_{AR}	9.2	A
Repetitive Avalanche Energya	E_{AR}	6.0	mJ
Maximum Power Dissipation ($T_C = 25$ °C)	P_D	60	W
Peak Diode Recovery	dV/dt	5.5	V/ns
Operating Junction and Storage Temperature Range	T_J, T_{stg}	- 55 to + 175	°C
Soldering Recommendations (Peak Temperature) for 10 s		300	°C
Mounting Torque (M3 screw)		1.1	Nm

Table 3.12: Absolute Maximum Ratings of the IRF520 Power Mosfet

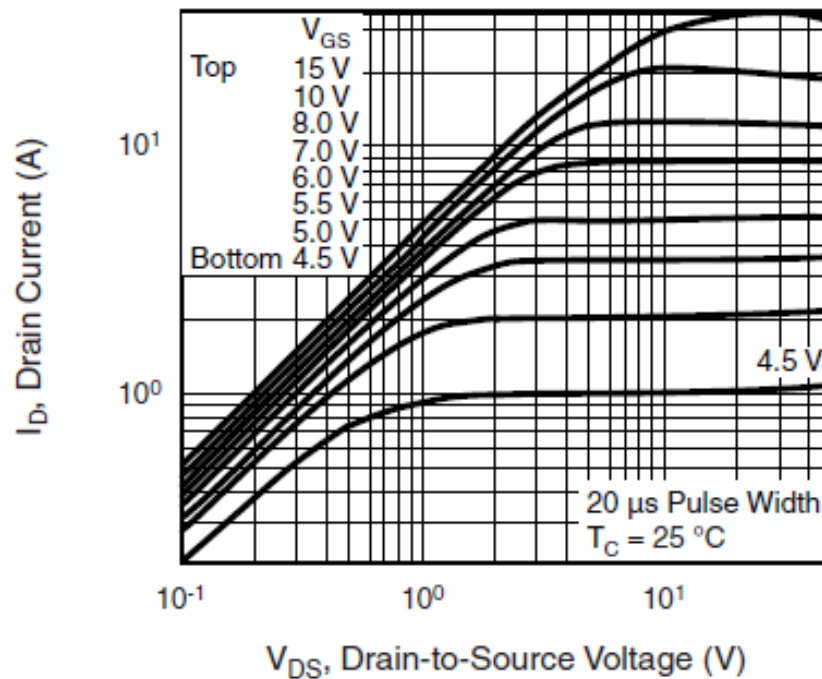


Figure 3.17: IRF520 Power Mosfet Characteristic at 25°C

3.4.5 Arduino UNO Electric Supply Power

The electric power to the system is guaranteed by the regulated power supply, which is able to provide a maximum current of 2 A for each channel. The electric power to the Arduino board is provided through the USB cable which is used also to allow communication between the Arduino itself and the computer used to generate the command signal via MABATLAB[®].

3.4.6 Response to the Command Signal

In the figure 3.18 it can be seen an example of what happens to the sensed temperature in the isolated volume when a step command temperature of 30, 40, 50 °C with 30 seconds in duration for each step is considered.

The MATLAB[®]platform is used to generate the command step signal. This last is a very precise signal because it exploits the computer clock signal to compute the time, so the instants where the signal configuration must change. The sensed temperature signal also is sent back to the computer in the MATLAB[®]platform and could be plotted as seen in figure 3.18.

Obviously, when a change in the control temperature occurs, an overshoot occurs in the temperature signal detected before the temperature is stabilized by the controller. After that, the integrative control loop brings the average temperature value to the command temperature value.

Once built the temperature control system, is time to collect some information about what happens to the optical fiber, which is in the same isolated volume as the temperature sensor.

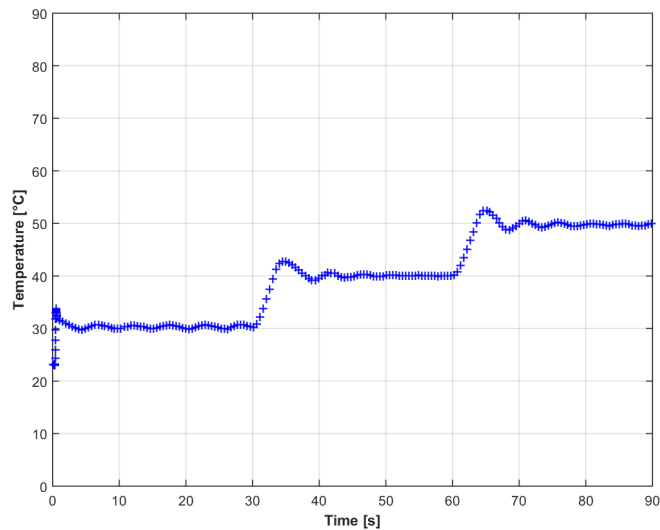


Figure 3.18: Example of a Command Response

In the figure 3.19 below it can be seen a preliminary test of the command system.



Figure 3.19: Command Test

3.5 Optical Signal Acquisition System

3.5.1 Introduction

The optical signal acquisition system has the objective to collect data from the optical fiber and to provide it to the computer, so they can be post-processed.

The optical fiber is installed in the isolated volume and collects data related to this temperature controlled environment.

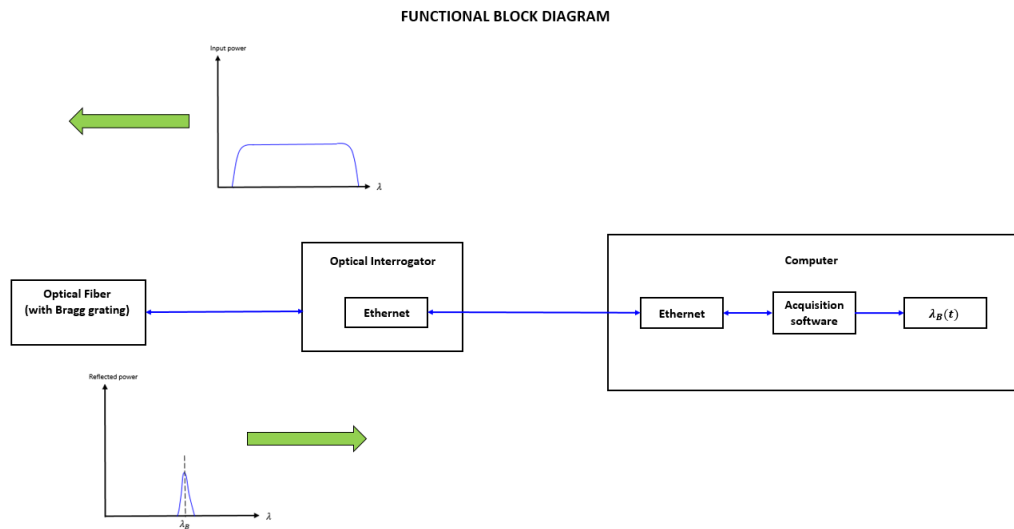


Figure 3.20: Optical Signal Acquisition System

How can be seen from figure 3.20 the core of the data collecting is the *Optical Interrogator*. In this figure is reported the functional block diagram of the optical signal acquisition system, considering only one channel of communication and only one Bragg grating, to simplify the approach.

The main functions of an optical interrogator are:

- Send a interrogation broadband signal through the optical fiber
- Be able to detect the reflected signal coming from the Bragg grating
- Be able to detect the Bragg wavelengths
- Be able to convert the optical data into digital data
- Be able to communicate with the external devices

Once that the information has been sent to the computer, via Ethernet, then it can be processed or stored into a text file using the acquisition software. This information will contain the measured Bragg wavelengths and the target times where these measurements took place.

3.5.2 FBG Interrogator

The optical FBG interrogator used is reported in figure 3.21, and its main characteristics are reported in table 3.13 and in table 3.14.



Figure 3.21: SmartScan FBG Interrogator

Parameter	Value	Unit
Wavelength Range	40 (1528 – 1568)	nm
Number of Optical Channels	1-4	
Bragg Grating Full Width Half Maximum (FWHM)	> 0.5	nm
Maximum Number of Sensors / Channel	16	
Scan Frequency (all sensors simultaneously)	2.5	kHz
Wavelength Stability	< $\pm 5 \pm 20$ over 25 years	pm
Dynamic Range	27	dB

Table 3.13: SmartScan FBG Interrogator: Main Measurement and Processing Specifications

If one looks to the table 3.13, the first parameter described is the *Wavelength Range*. This is very important because indicates the extremes of the broadband signal range read by the optical interrogator. This means that if one wants the signal to pass through a Bragg grating which has a reflected wavelength not included in that interval, no reflected signal is captured by the optical interrogator.

The choice of the optical fiber must so respect the optical interrogator range characteristic.

Parameter/Object	Value/Description
Dimensions	140 x 110 x 70 mm
Weight	0.9 kg
Operating Temperature	-20 to 60 °C
Comms Interface Ethernet	UDP-UP
Data Connector	RJ45 standard
Optical Connectors	FC/APC 2.5 mm <small>Ferrule Diameter</small>
Input Voltage	+9 to +36 VDC
Power Consumption	typ 7.5W, max 10W

Table 3.14: SmartScan FBG Interrogator: Mechanical, Environmental and Electrical Specifications

3.5.3 Optical Fiber

The optical fiber and its relative grating used to sense the temperature have the characteristics reported in table 3.15 and table 3.16. The *Center Wavelength* is the main characteristic of the optical acquisition system. It is reported in table 3.16. The commercial name of the system is *FemtoFiberTec GmbH - Am Stollen 19 - 38640 Goslar*

Provided by	Manufact.	Fiber type	ϕ Core [μm]	ϕ Cladding [μm]	Coating	Fiber length [m]
FFT	Fibercore	SM1250BI	9.8	125	Polyimide	2,000

Table 3.15: Fiber Specification

Grating No.	Position [m]	Center Wavelength [μm]	FBG length [mm]	Reflectivity [%]	3dB Bdwd [nm]	SNR [dB]
1	1.0000	1560.09	3.2	74.8	0.48	25.1

Table 3.16: Grating Specification at 21 °C - Measurement Equipment: YOKOGAWA AQ637D

3.5.4 Acquisition Software

The acquisition software provided by the FBG interrogator constructor has got a graphic interface to set the parameters of the acquisition and data handling. It shows also the Bragg wavelength in real time. An example of what happens on the computer screen can be seen in figure 3.22.

In the same figure, it is possible to see the reflected signal from the Bragg grating. a inner function of the data handling system is able to detect the center wavelength of the reflected spectrum, which is the Bragg wavelength. This is the wavelength with the maximum relative intensity respect to the signal sent by the optical interrogator.

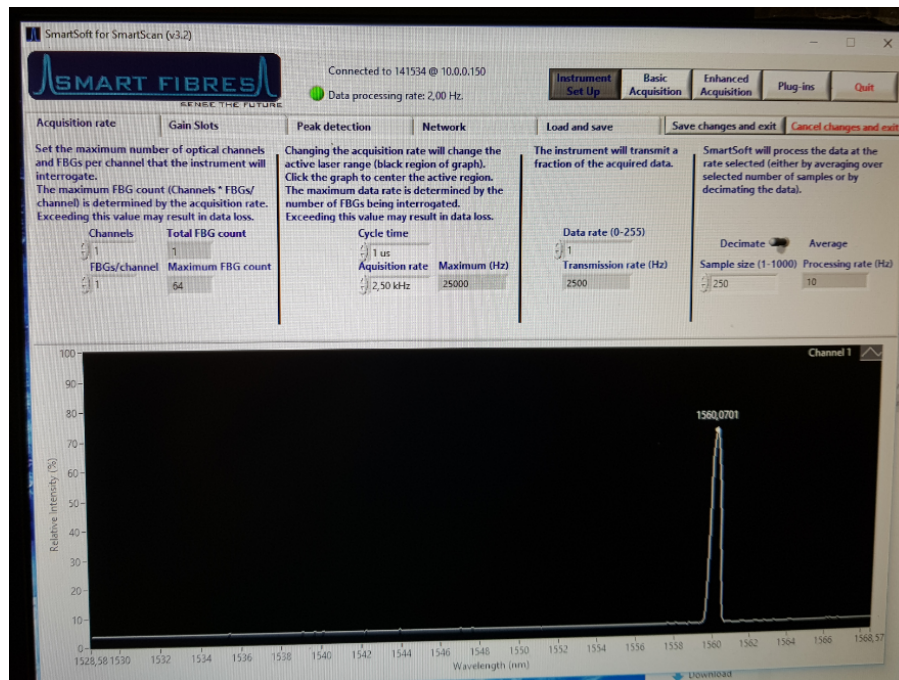


Figure 3.22: SmartScan FBG Interrogator Software Interface

3.6 Test Bench Operation and Functional Block Diagram

Once the temperature control system has been made, the optical fiber is installed in the isolated volume. This is the final step to build the test bench. The optical system illustrated in figure 3.20 must be connected to the computer; at the same time the command temperature system illustrated in the figure 3.10 must also be connected to the computer. Another thing to do is to provide the sensed temperature to the computer to be able to plot its variation over time. The result of the whole installation can be seen in figure 3.23 illustrated below:

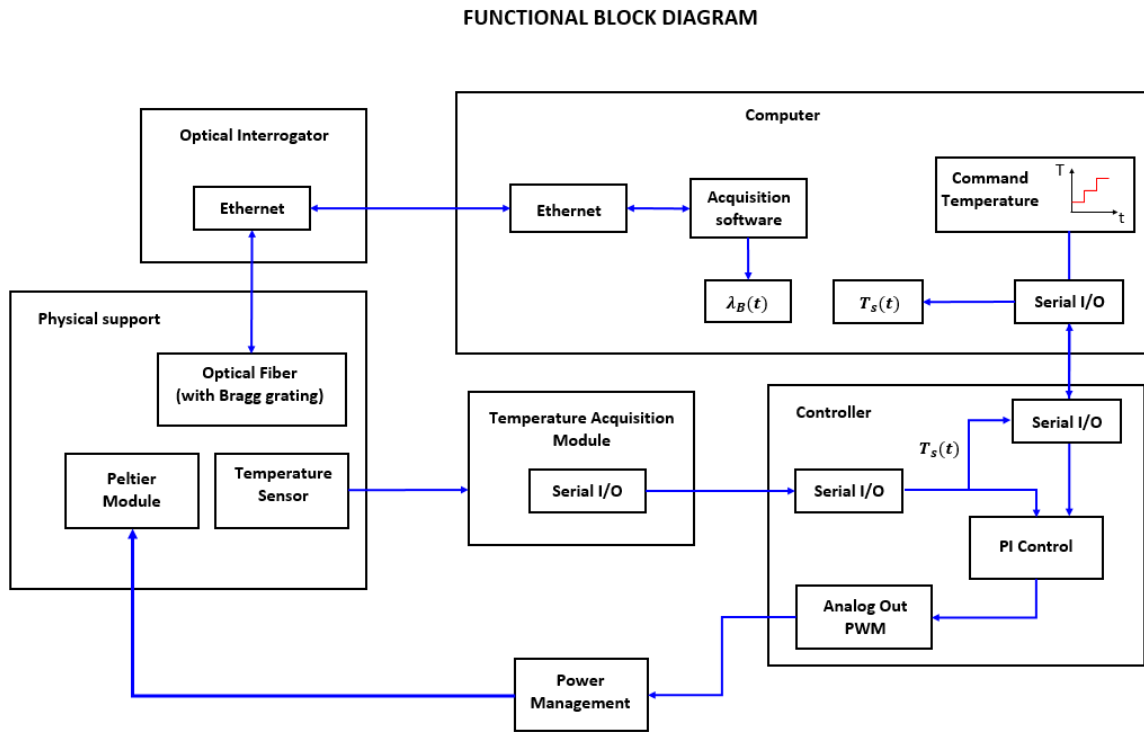


Figure 3.23: Test Bench Functional Block Diagram

Chapter 4

Data Collection and Post-Processing

4.1 Introduction

If one want to build a temperature sensor using the optical fiber, obviously it is necessary to observe the behavior of the optical fiber when the temperature changes.

So, the first thing to do is to provide the most wide possible temperature range in order to capture the phenomenon. Since that the control takes time to stabilize the temperature around a certain value, one can command a step temperature signal. This is useful also to have a lot of measurements for each commanded temperature value.

The command temperature signal must also respect the limit values of the Peltier Cell. These values are reported in table 3.5. In particular, the command temperature signal must not exceed the operative temperature ranges of the Peltier module.

Once these considerations have been done, it can be chosen the command temperature signal to be followed by the controller.

4.2 Command Temperature Signal Setup

The command temperature signal chosen is a 10°C steps temperature signal, from 30 to 80 °C. Each step is 60 seconds in duration. Obviously also the ambient temperature must be considered, because is not possible to get a lower temperature with this system configuration. In reality one could invert the Peltier Cell polarity and so the cold side will be in contact with the sensors, but the hot side must have some heat exchanger to dissipate the thermic power from the cold side to the external environment. In that way one will be able to do a cryogenic test. However, in the examined case the fiber calibration will be done for positive temperature variations.

In the figure 4.1 below it is possible to see the command temperature signal that will be used to test the fiber.

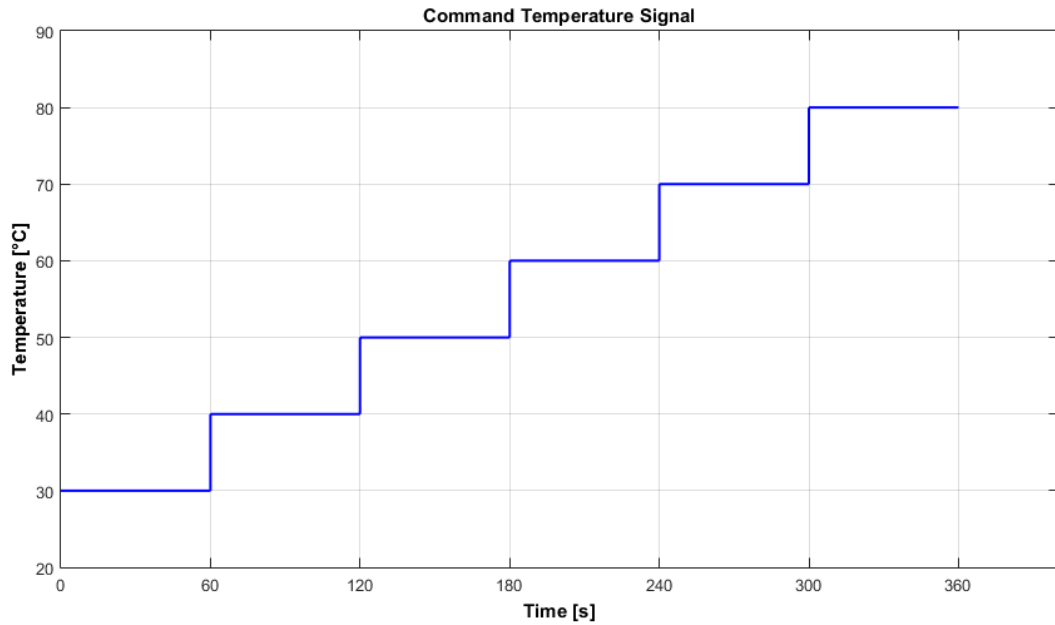


Figure 4.1: Command Temperature Signal

4.3 Sensed Temperature in the Isolated Volume

Before testing the fiber, is convenient to test what happens in the isolated volume. The sensed temperature signal coming from the Pt-100 temperature sensor is used to analyze the temperature trend over time.

One expects that the response of the system will be like the one described in 3.4.6. But in that case the maximum commanded temperature was not very high: it was 50 °C, how can be seen looking to the figure 3.18.

In a wide temperature range perspective, the isolation provided by the physical support begins to have more importance to help the system to maintain a certain temperature, mostly when the temperature values start rising.

If the system is well isolated, which means that:

- The system is correctly mounted
- The sensors are well positioned and in contact with the Peltier cell
- The tightening torque of the mechanical connections is adequate
- The pressor acts correctly on the gasket, and this last on the sensors

Then the sensed temperature will be the same as the commanded when the commanded temperature is high.

In the figure 4.2 below it is possible to see what happens to the sensed temperature when the command temperature signal in figure 4.1 is set up and the system is well isolated.

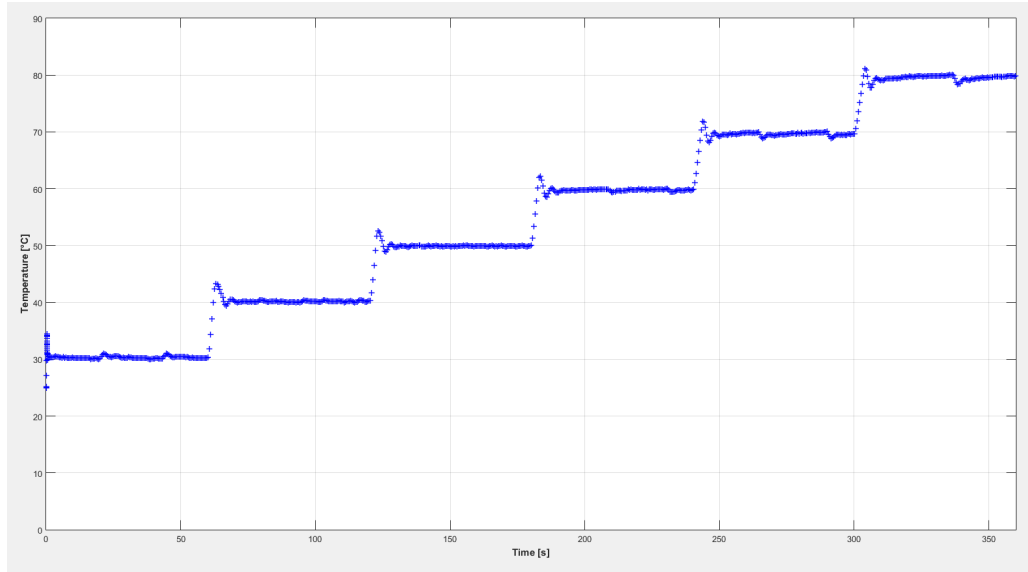


Figure 4.2: Sensed Temperature Signal, system well isolated

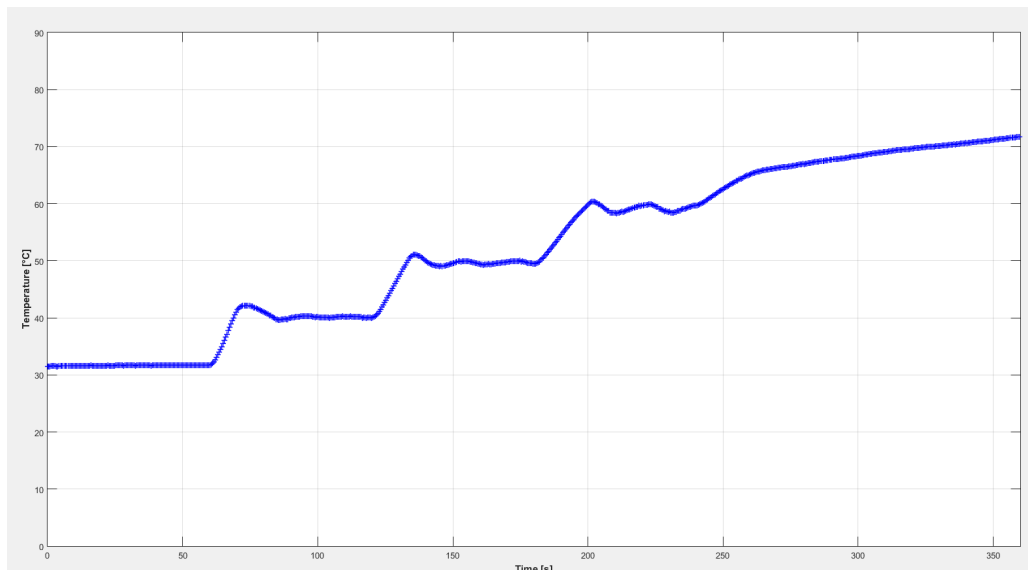


Figure 4.3: Sensed Temperature Signal, system badly isolated

An example of what happens when the system is badly isolated can be seen in the figure 4.3. One can observe the loss of signal stability and the impossibility to reach high temperature values.

Once ascertained that the temperature control works properly, especially at high temperatures, than the optical fiber can be installed in the isolated volume together with the Pt-100 sensor.

In the figure 4.4 it is possible to see the optical signal acquisition system. It is composed by the optical interrogator, the optical fiber connected to the channel 1 of the same interrogator, the DC Power Supply and the Ethernet cable to communicate with the computer by the acquisition software.

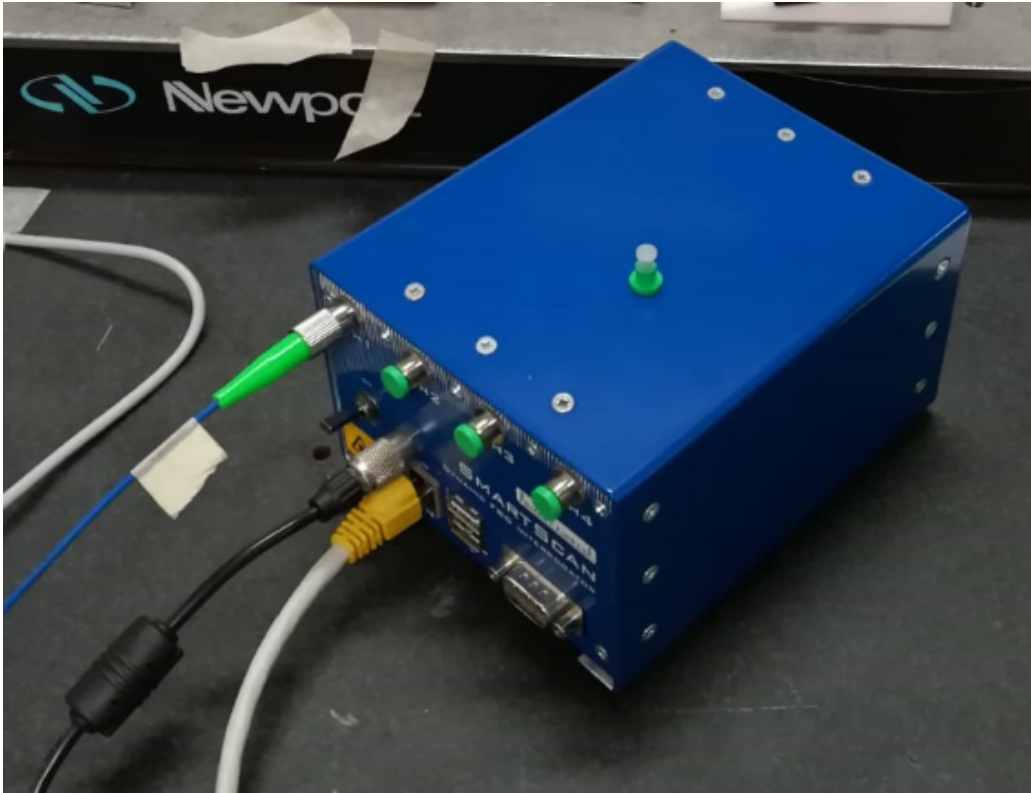


Figure 4.4: Optical Signal Acquisition System

Now it is possible to get the two signals and make a comparison. One is the signal which comes from the Pt-100 sensor and the other is the signal which comes from the optical interrogator. So a temperature signal and a wavelength signal are compared. The goal is to transform the signal which comes from the optical fiber in order to have a temperature signal. This is the first step that will allow to build a temperature sensor using the optical fiber technology.

4.4 Optical Fiber and Pt-100 Sensor: Signal Comparison

4.4.1 Introduction

Once that the command signal in figure 4.1 has been set up, the sensed temperature signal is sent to the computer. Meanwhile, the optical fiber signal is also sent to the computer.

Obviously, these two signals are not in phase. This is due to various factors like for example the different acquisition speed of the two systems, the different starting time of the two acquisitions and the delay time of the Pt-100 sensor, since the optical fiber response speed can be assumed as the speed of light.

Since the signals present some overshoot peaks due to the temperature control system, these ones can be used to put in phase the two signals: in this way the two signals will be referred to the same time. The result of that process provides the situation illustrated in figure 4.5 below:

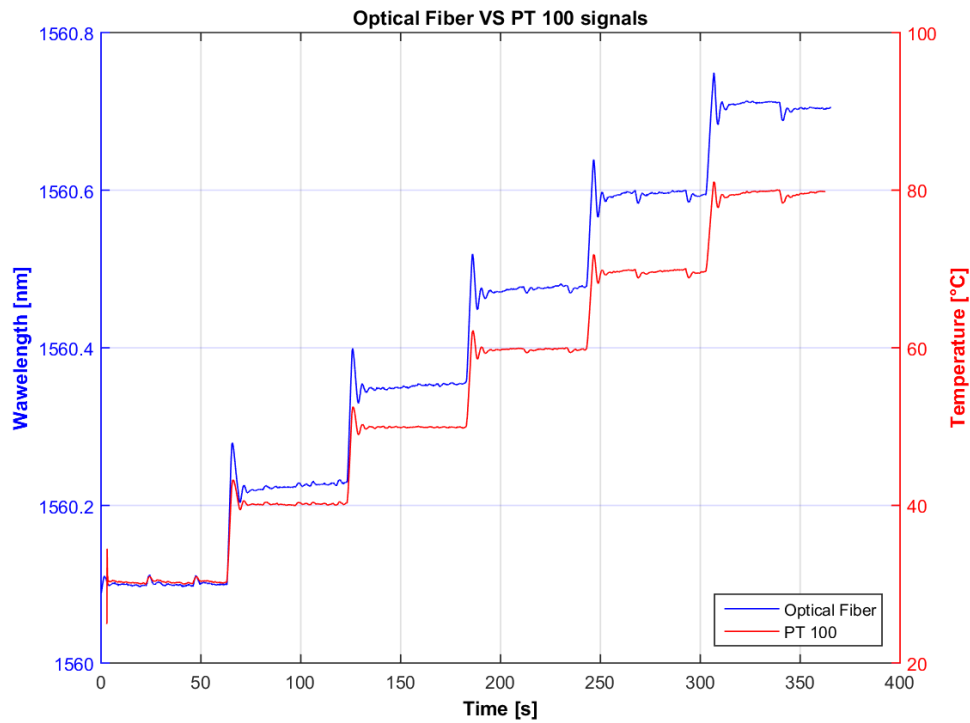


Figure 4.5: Optical Fiber VS Pt-100 Signals

The shape of the two signal is similar, and this can be considered as a good result to start some consideration. Before doing that, one can observe the limit values of the two dimensions.

The temperature rises up from the room temperature to about 80 °C. Meanwhile, the optical fiber grating reflects a wavelength that doesn't change more than a 1/10 of a nanometer. This is a very small variation. It can be considered as a second order effects measurable by the optical fiber. An appreciable variation of the Bragg wavelength occurs when the fiber is subjected to mechanical deformation.

This is connected to the fact that if the mechanical deformation mostly acts on the grating period, the temperature acts mainly on the refraction index of the system.

4.4.2 Useful Measurements

The measurements of interest are that points of the steps far from the transient region, where overshoot peaks occur. Obviously, the time step considered must be the same for the two signals, in order to have the best result. For each temperature step considered, there will be a corresponding wavelength step. Each step is composed by a series of measurements done by the two tools in the interval time considered.

In the figure 4.6 and figure 4.7 it is possible to see the measurements considered. The overshoot peaks are isolated and also are not considered the extra data of the signals due to the in phase putting and to the acquisition processes ending time.

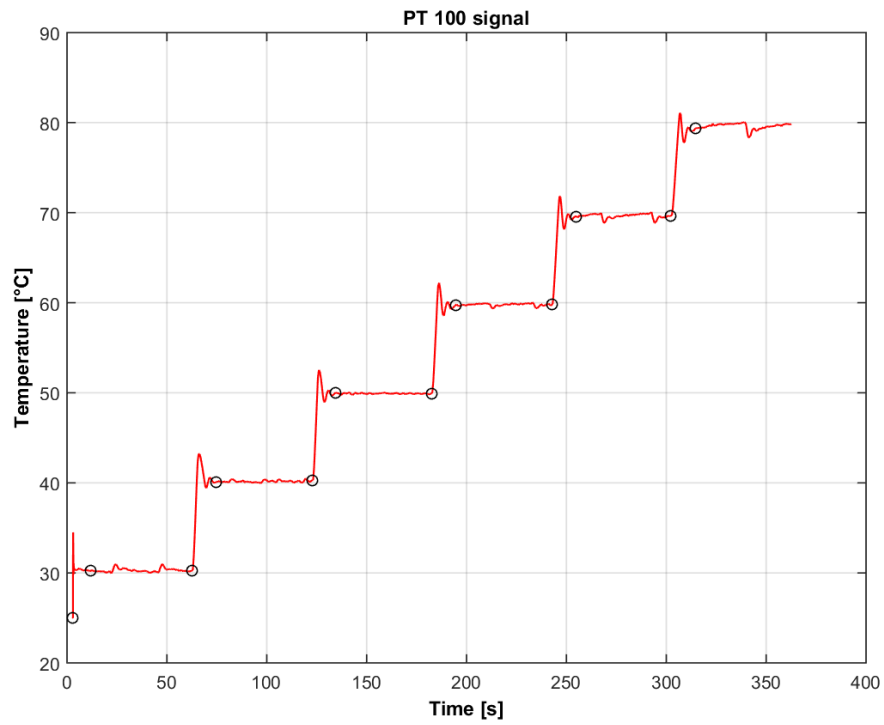


Figure 4.6: Pt-100 Signal - Overshoot Peaks Isolation

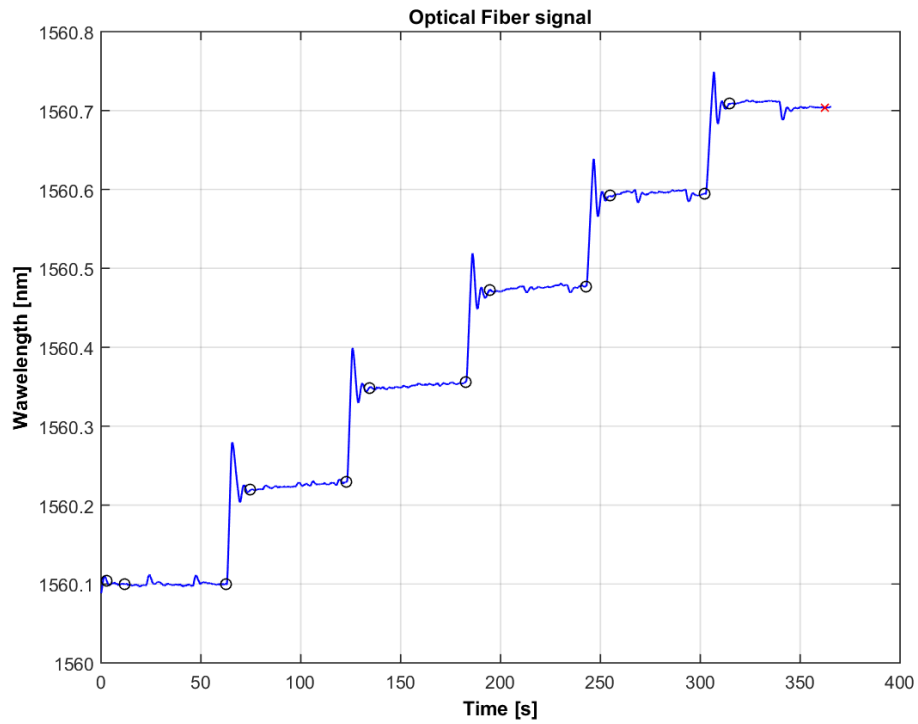


Figure 4.7: Optical Fiber Signal - Overshoot Peaks Isolation

4.4.3 Interpolation

Since every step considered contains a lot of measurements, a mean value for each step of the two signals over time was done. The resulting interpolation can be seen in figure 4.8. In this case a first order interpolation was done to find the sensed temperature trend as a function of the wavelength measured by the optical fiber. The developed software is able to interpolate with higher polynomial degree, but from the mentioned figure above it can be seen that the linear interpolation is good.

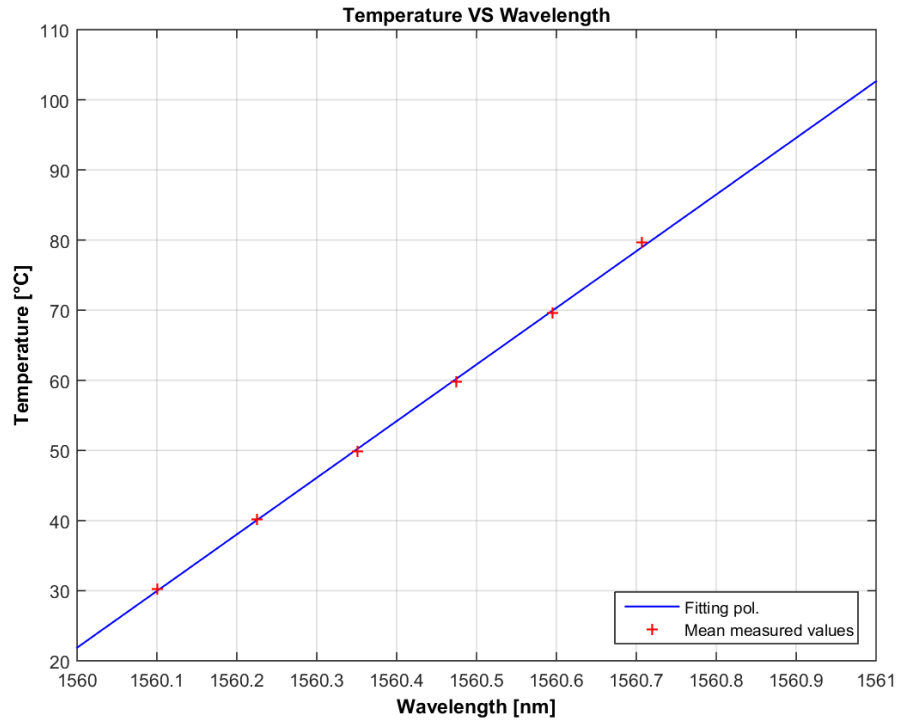


Figure 4.8: Data Interpolation

Let consider a polynomial that describe the sensed temperature in function of the measured wavelength like:

$$T(w) = t_1w^n + t_2w^{n-1} + \dots + t_nw + t_{n+1} \quad (4.1)$$

For a linear interpolation and considering the above conditions, the coefficients of the polynomial interpolation are reported below, in descending powers:

- $t_1 = 80.7599 \frac{^{\circ}C}{nm}$
- $t_2 = -1.259635739 \cdot 10^5 \text{ } ^{\circ}C$

Thanks to this operation, it is possible to transform the wavelength signal coming from the fiber

to a temperature signal. In this way the optical fiber is calibrated to function as a temperature sensor.

Obviously, if the boundary conditions change, for example if the system is disassembled and reassembled, the above mentioned coefficients also change. It would therefore be necessary to recreate the identical assembly conditions to have two identical tests.

Once the fiber is mounted and fixed definitely to a system, the calibration will be also definitive.

4.4.4 Sensed Temperature

Once that the wavelength signal is transformed into a temperature signal, it is possible to compare the two signals. Each signal will be referred to the sensed temperature. The result of this transformation can be seen in figure 4.9 below.

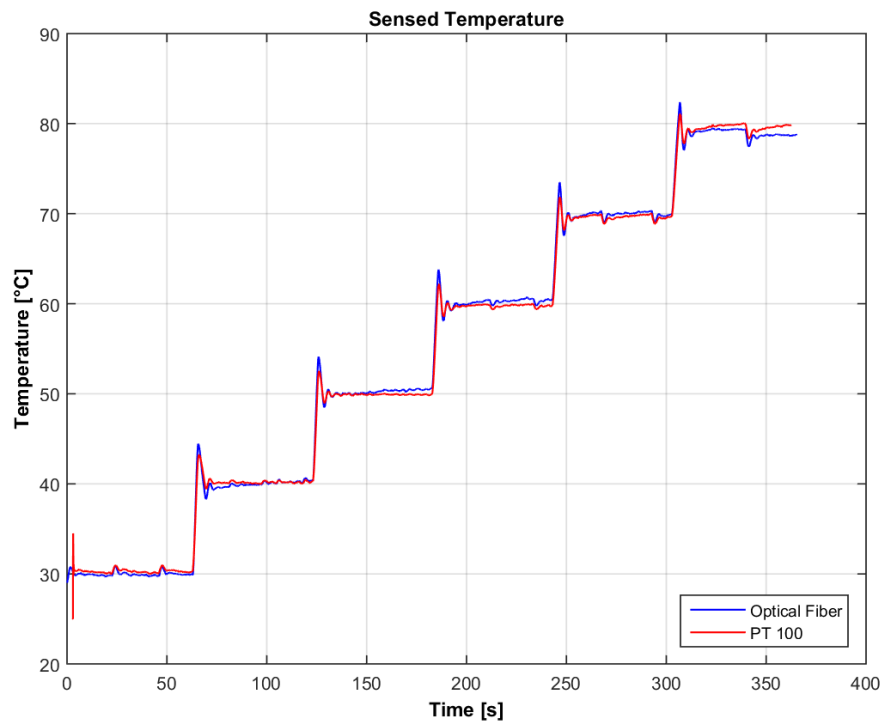


Figure 4.9: Optical Fiber VS Pt-100 Signals: Sensed Temperature

From the same figure one can see that the sensed temperature of the optical fiber is with a good approximation identical to the one measured by the Pt-100 sensor.

Now it is possible to develop a temperature sensor based on the fiber optical technology, with all the advantages that this entails like the high response speed of the sensor. There is also the possibility to fix it to the electric motors coils, since it has a very small volume and it doesn't suffer electromagnetic fields interference. In this way one can get a high performance control of the electric motors, allowing them to reach the limit performance.

Chapter 5

Construction of a Temperature Sensor with Optical Fibers

5.1 Introduction

If one would to build a real time temperature sensor, the previous steps can be used. The difference is how the data are handled. Now there is the need to manage the information at the maximum speed and provide it to the computer. This real time signal will then be used to control a system or in general to read the actual temperature value of a certain point.

5.2 Acquisition and Data Handling Software

The real time acquisition software used was developed in a previous work done by Mauro Guerrero, *Algorithms and Methods for Fiber Bragg Gratings Sensor Networks*. In this paragraph will be explained the main features of this software and how it can be integrated in order to provide a real time temperature signal available on the cloud.

The aim of this work was to create a complete and scalable software architecture for a generic system that integrates a set of FBG sensors. The architecture is required as a part of the PhotoNext group research project regarding FBG technology and system monitoring.

Most applications depend on dedicated and usually closed-source software platforms. There is also a lack of an integrated system that allows to directly read data from FBG sensors and convert it into a visually effective representation.

In order to provide a seamless integration of these sensors into a *Internet of Things* platform, a new architecture has been designed and deployed, implementing a full software stack able to interface with a generic interrogator. The architecture features a middleware layer that collects data and forwards it to a low latency cloud database.

Furthermore, the platform includes a AR/VR system to visualise data collected from sensors. The implementation is fully open source and integrates some popular and well tested third-party open source software.

The software rely on a *Middleware Layer* and a *Cloud Network Services Layer*.

The main function provided by the Middleware Layer is to bring IoT connectivity to the interrogator module. It also hides details about the physical interrogator and it is used as an abstraction layer that is directly interfaced to the cloud storage network. The middleware provides also an additional security layer, by establishing an encrypted connection to the data server.

The Cloud Network Services Layer stores data coming from the middleware client, performs a first analysis on raw peak values and exposes a set of APIs to extract and manipulate data by a third party registered application. The KaaIoT platform architecture was chosen. The main features of this IoT technology framework (open source, flexibility, built-in security, scalability) make it a perfectly suitable candidate for the implementation of the cloud network services layer.

The *Smartfibres*[©] Smartscan behaviour has been analysed to create a custom C++ interface library, which can be used by the upper middleware layer of the framework to extract data from the Smartscan interrogator and to set the interrogator parameters and the communication parameters.

In this work was chosen to built only a temperature sensor, but the described architecture could be developed in a future work.

If one has to manage some data from C++ Platform to for example MATLAB[®], there are some libraries to send the data. These libraries depends on the version of the software used and are a limit if one want to build an high compatibility platform.

So in this case the middleware layer is used only to set the FBG interrogator. The data are then got directly using MATLAB[®]. In a future develop the interface with the cloud will allow the data to be handled by every platform, simply using a communication protocol.

In the work of this thesis, the software was modified and simplified for this case study. The main purpose is to read the temperature value in real time. One is able to do that using the C++ software (middleware layer) to set the FBG interrogator and for example MATLAB[®] to get, store and handle the data and finally plot the sensed temperature value measured by the optical fiber.

In the figure 5.1 below it is possible to see how the acquisition and real time data handling is performed.

In a future development, with the implementation of a Cloud Network Service Layer, the data will be available on the cloud and could be shared also with other devices, in the optic of IoT connectivity.

In the figure 5.2 below it is possible to see an example of how the acquisition and real time data handling could be performed in the next upgrade of this work. Moreover, it is possible to by-pass the MATLAB[®] platform and use a commercial software to handle the data. In this last case, the algorithms used to calibrate the fiber and for data handling have to be developed in the new platform.

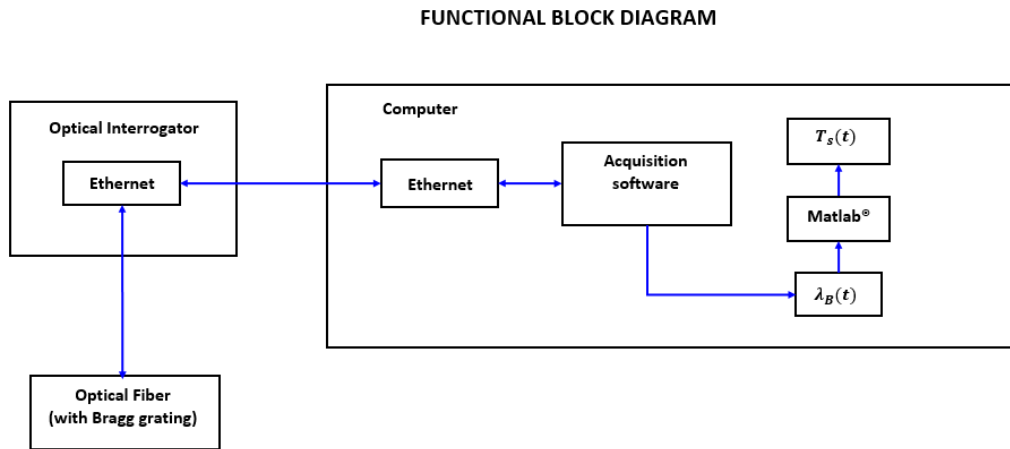


Figure 5.1: Acquisition and Data Handling Functional Block Diagram

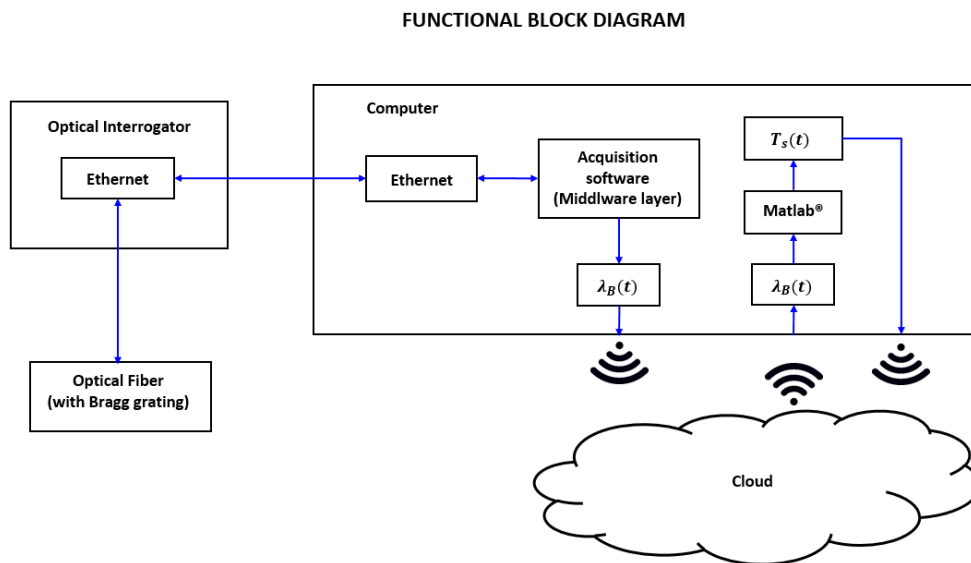


Figure 5.2: Future Develop: Acquisition and Data Handling Functional Block Diagram

5.3 Conclusions

The MATLAB[®] platform is not optimized to perform at very high speed with the UDP protocol. So a new platform has to be considered. The system works really well on the C++ platform, with a total delay time of 1 ms for each data transmission from the FBG interrogator. One can plot these data using directly this platform or sending the data for example to the LabVIEW Platform. It was implemented the MATLAB[®] platform because many students are able to use it well. But the delay time due to the acquisition function *fget* rises up to 200 ms.

Appendix A

Develop of a Control System for a Servo Motorized Micrometer Head

Introduction

This control system is developed for the Alice Sgroi project and allows to deform the optical fiber along its axis. The deformation is imposed by the fiber displacement which is controlled by the servo motorized micrometer head.

The goal is to study how varies the Bragg Wavelength with the FBG deformation. This allows also to find the law to measure the deformation in function of the Bragg Wavelength.

In the pages below are described the components used. The controller [3.15](#), the power supply [3.7](#) and the optical interrogator [3.21](#) are the same used in the work of this thesis. Also the response to the command signal is managed in the same way.

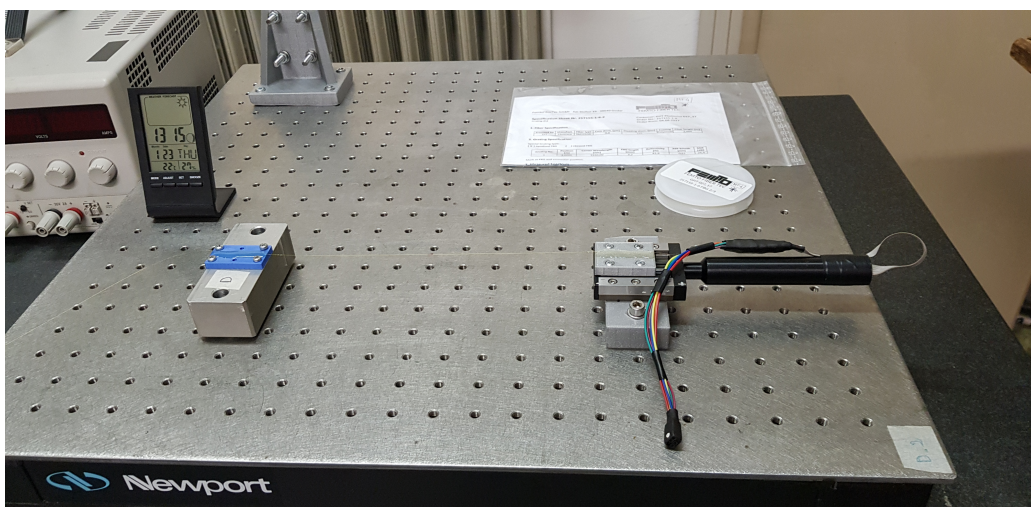


Figure 5.3: Tensioning of the Optical Fiber with the Servo Motorized Micrometer Head

Components

Servo Motorized Micrometer Head

The TMS-16 servo motorized micrometer head has a 8V brushed DC gearmotor and a 3922 steps TTL Magnetic encoder. The screwed spindle and nut has a pitch of 0.5 mm per revolution.

Model	Stroke [mm]	Speed [mm/s]	Accel. [mm/s ²]	Resolution [μm]	Accuracy [μm]
TMS-16	16	0.2	0.2	1	±3

Table 5.1: TMS-16 Servo Motorized Micrometer Head Charateristics

H-Bridge

The H-Bridge is a circuit that allows to invert to DC motor polarity so one can move the micrometer head in any direction. In this case it was chosen a integrated circuit: SN754410 Quadruple Half-H Driver.

The SN754410 is a quadruple high-current half-H driver designed to provide bidirectional drive currents up to 1 A at voltages from 4.5 V to 36 V. The device is designed to drive inductive loads such as relays solenoids, DC and bipolar stepping motors, as well as other high-current/high-voltage loads in positive supply applications.

All inputs are compatible with TTL-and low-level CMOS logic. Each output (Y) is a complete totem pole driver with a Darlington transistor sink and a pseudo-Darlington source. Drivers are enabled in pairs with drivers 1 and 2 enabled by 1,2EN and drivers 3 and 4 enabled by 3,4EN. When an enable input is high, the associated drivers are enabled and their outputs become active and in phase with their inputs. When the enable input is low, those drivers are disabled and their outputs are off and in a high impedance state. With the proper data inputs, each pair of drivers form a full-H (or bridge) reversible drive suitable for solenoid or motor applications. A separate supply voltage (V_{CC1}) is provided for the logic input circuits to minimize device power dissipation. Supply voltage V_{CC2} is used for the output circuits.

The SN754410 is designed for operation from -40°C to 85°C .

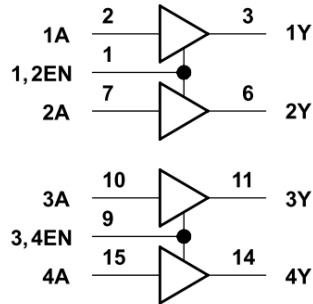
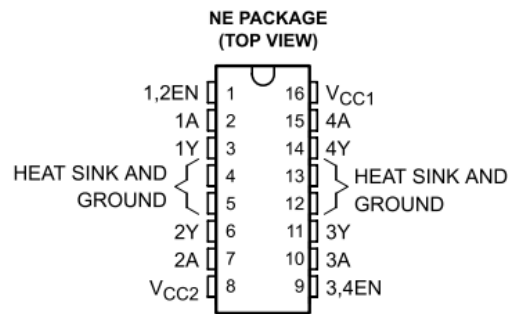


Figure 5.4: SN754410 H-Bridge Simplified Schematic



Pin Functions

PIN		TYPE	DESCRIPTION
NAME	NO.		
1,2EN	1	I	Enable driver channels 1 and 2 (active high input)
<1:4>A	2, 7, 10, 15	I	Driver inputs, non-inverting
<1:4>Y	3, 6, 11, 14	O	Driver outputs
GROUND	4, 5, 12, 13	—	Device ground and heat sink pin. Connect to circuit board ground plane with multiple solid vias
V _{CC2}	8	—	Power VCC for drivers 4.5V to 36V
3,4EN	9	I	Enable driver channels 3 and 4 (active high input)
V _{CC1}	16	—	5V supply for internal logic translation

Figure 5.5: SN754410 H-Bridge Pin Configuration and Functions

Functional Block Diagram

The data acquisition system is very similar to the one made in this thesis. The control loop has also a derivative control loop, which contains also a filter to avoid the noise related interference.

The integrative and derivative control loops are also saturated to avoid overflow, since a certain number of bit can be used to memorize a maximum finite integer value which is 2 elevated to the number of bits used to store the information.

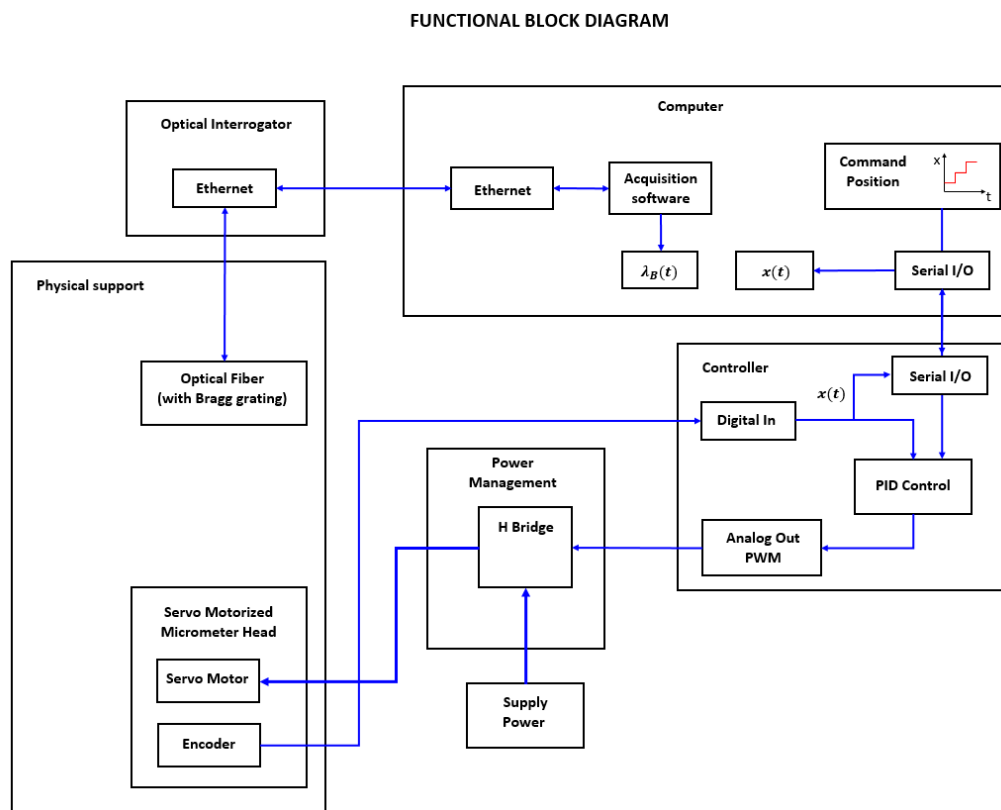


Figure 5.6: Data Acquisition and Position Control System - Servo Motorized Micrometer Head

The serial communication protocol is described in the table below:

Between the encoder pins and the ground are installed 10 nF condensators to avoid false contacts. This is called de-bounce circuit.

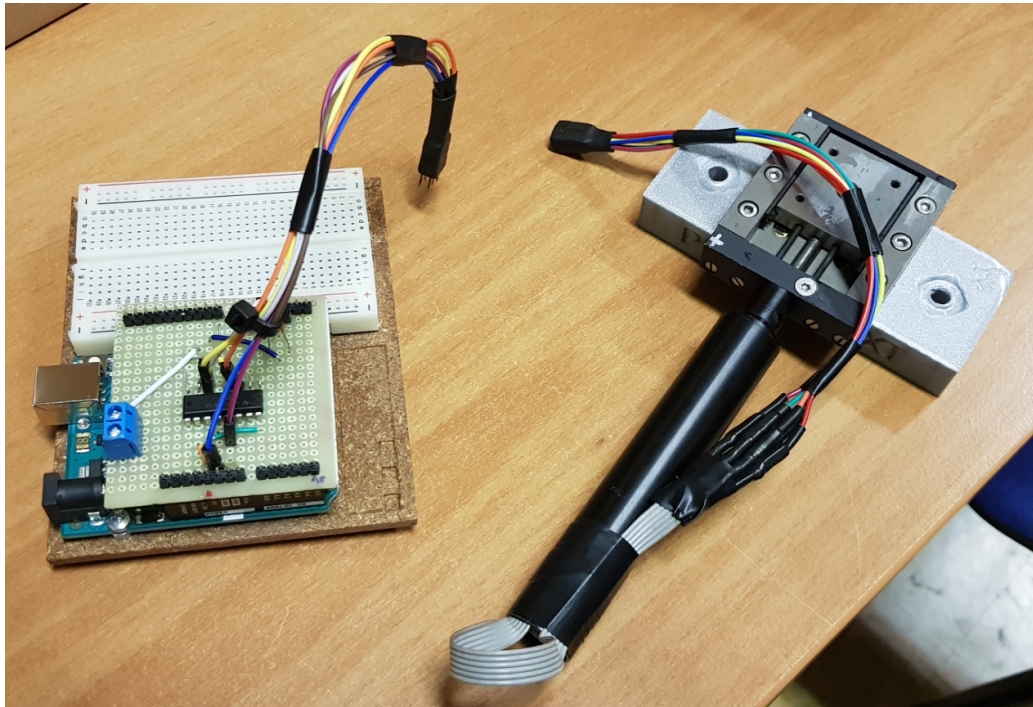


Figure 5.7: Controller with related electronics and Servo Motorized Micrometer Head

Parameter	Value
Start Bit	1
Data Bits	8
Parity Bits	0
Stop Bits	1
Baud Rate	9600 bit/s

Table 5.2: Serial Communication Protocol - MATLAB

Pin	number
Encoder A	2
Encoder B	4
Motor Enable	6
Motor +	7
Motor -	8
Ground	

Table 5.3: Arduino Pinout

In figure 5.8 it is possible to see the response of the servo mechanism to a command position step signal. The steps are 0.05 mm every 20 s. The position goes from 0 to 0.5 mm. This command step will be used to allow tensioning of the optical fiber. The zero position will be set with the pre-tensioned fiber. After this phase the test would start.

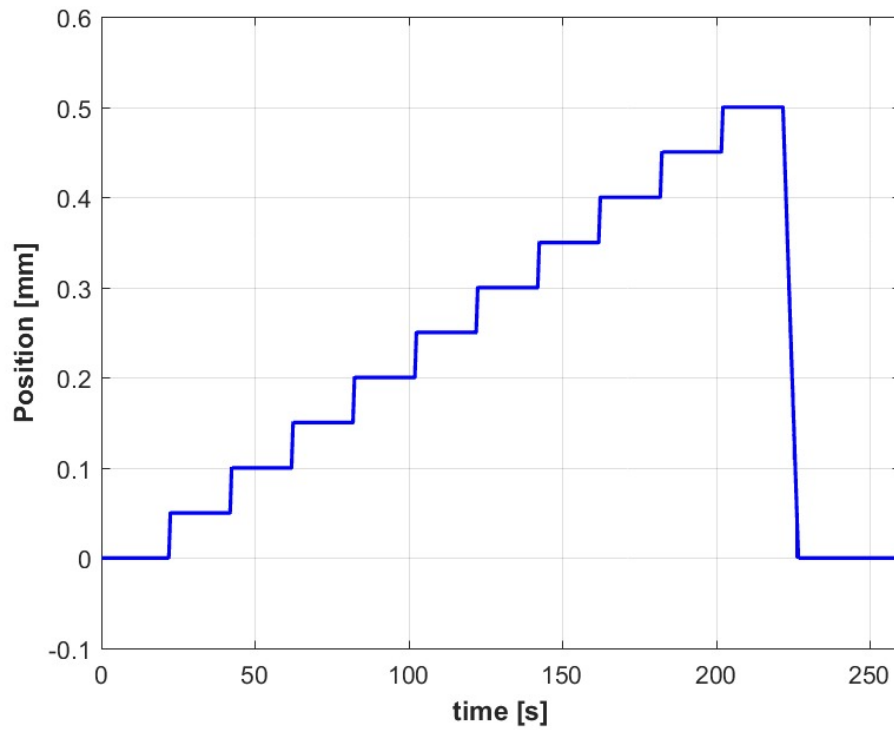


Figure 5.8: Example of a Command Response of the Servo Motorized Micrometer Head

Appendix B

Develop of a Servo Motorized Micrometer Head

Introduction

This control system is developed for the Bruno Lavagnino project and allows to deform an optical fiber glued on a spar, which is disposed as a cantilever beam. The deformation is imposed by the spar since this last is bended by the servo motorized micrometer head. The optical fiber is installed on the tensioned side.

The goal is to study how varies the Bragg wavelength with the free end displacement. This allows also to find the law to measure the deformation of the FBG in function of the free end displacement of the cantilever beam.

In figure 5.10 and in figure 5.11 respectively are reported the project and the final assembly of the servo mechanism. In the figure 5.9 it can be seen how the system works on the spar.

In the pages below are described the components used. The optical interrogator 3.21 is the same used in the work of this thesis. Also the response to the command signal is managed in the same way.

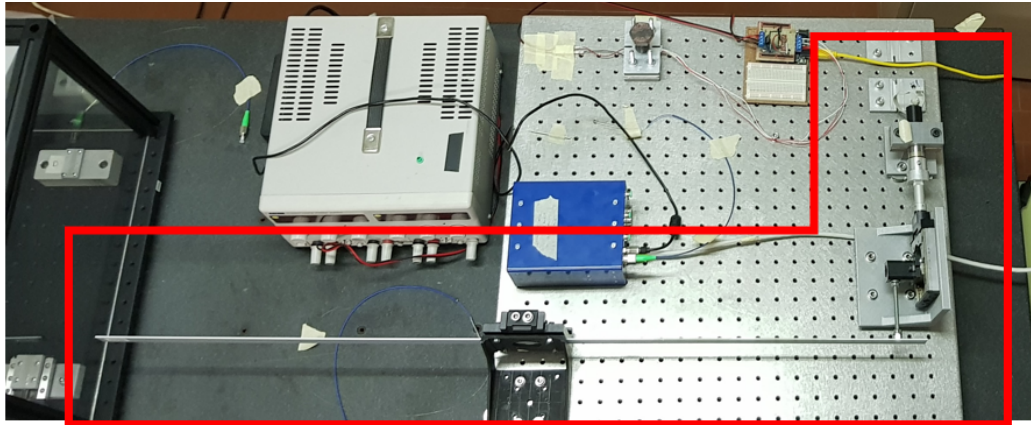


Figure 5.9: Servo Motorized Micrometer Head bending the spar

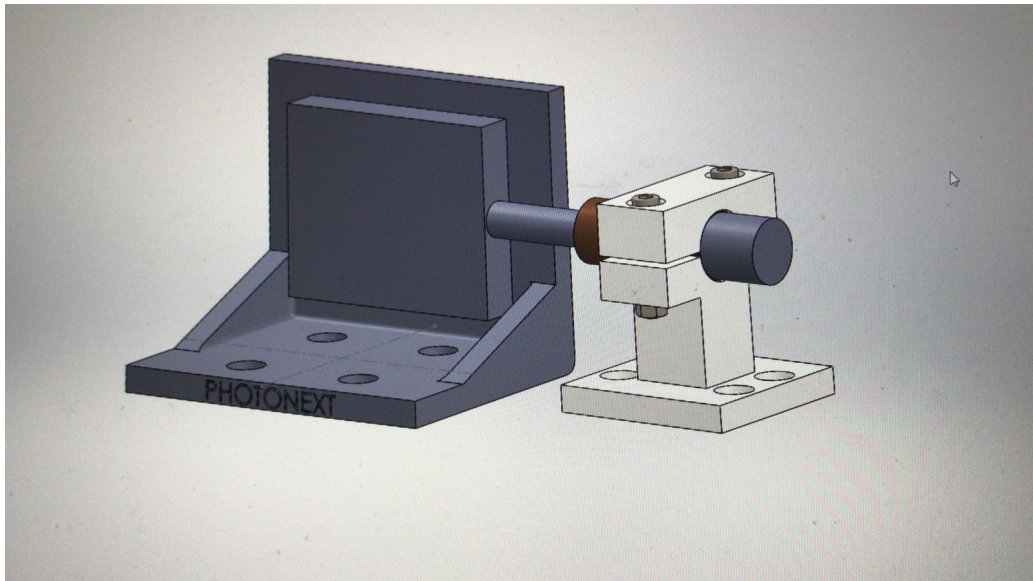


Figure 5.10: Servo Motorized Micrometer Head 3D CAD

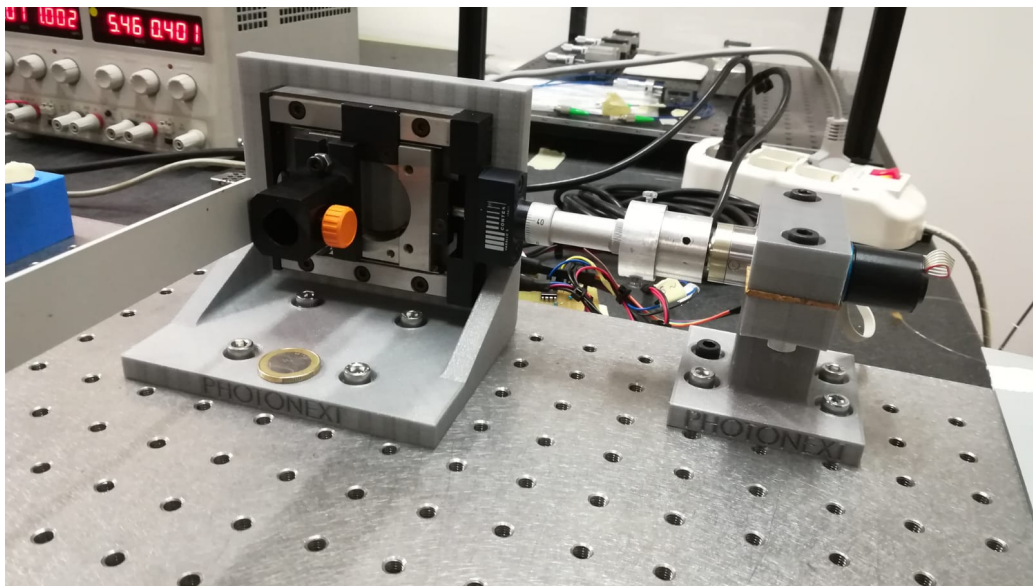


Figure 5.11: Servo Motorized Micrometer Head

Components

Physycal Support

The physical support is 3D printed, as can be seen in figure 5.11 This choice was the easy way to make the servo mechanism. The micrometer head plane is disposed to 90° angle with the Breadboard plane. The geramotor support must allow to the gearmotor to be in axe with the micrometer head and must equilibrate the torque reaction, which is very small considering that the micrometer head is a rolling guide.

Faulhaber Gearmotor with Magnetic TTL Encoder

The gearmotor moves the micrometer head. It was chosen this system because it was available from a previous project. The servo motor was equipped with the relative motion controller, even if no electric connections was available to allow the system to be plug and play.

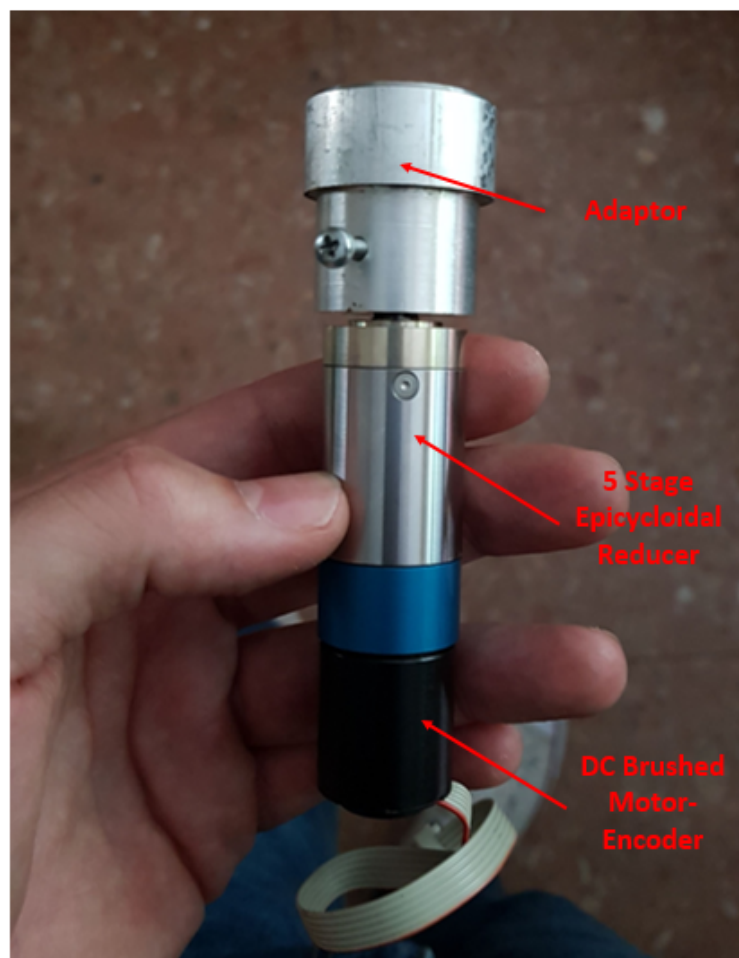


Figure 5.12: Faulhaber Epicycloidal Gearmotor with Adaptor for Micrometer Head

Parameter	value	Unit
Voltage	12	V
No-load speed	7800	min^{-1}
No-load Current	14	mA
Thermal Limit Current	520	mA
Max Current	1	A
Encoder lines per revolution	512	

Table 5.4: Faulhaber Series IE2-512 Precious Metals Brushed DC Motor with integrated Encoder - Main Characteristics

Parameter	value	Unit
Torque	0.7	Nm
Number of stages	5	
Transmission Ratio	592:1	

Table 5.5: Faulhaber Series 23/1 Planetary Gearhead - Main Characteristics

Micrometer Head and Adaptor

The adaptor transfers the torque from the reducer to the micrometer head. The micrometer head has a stroke of 25 mm and a pitch of 0.5 mm/rev.

So, considering also the parameters of the gearmotor, the servomechanism will have the characteristics reported in table 5.6.

Stroke	Speed	Resolution	Accuracy
$[mm]$	$[mm/s]$	$[\mu m]$	$[\mu m]$
25	0.11	0.2	$< \pm 3$

Table 5.6: Servo Motorized Micrometer Head Characteristics

Motion Controller

The motion controller acts as a controller, but integrates also the power management system, as can be seen in figure 5.13. In the figure 5.14 is reported the pinout. This controller communicates with the computer via RS-232 serial communication. The protocol is the same as reported in table 5.2.

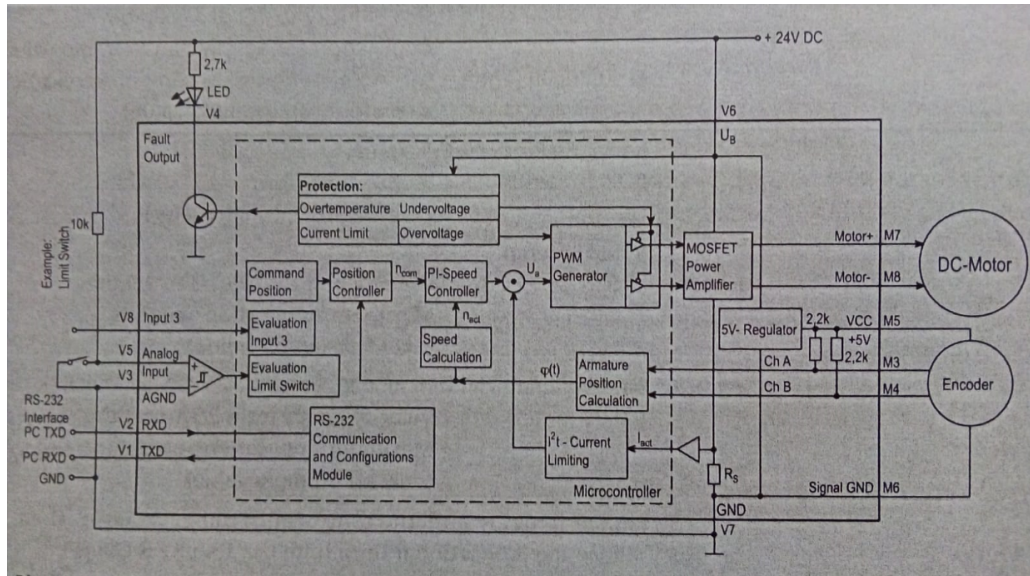


Figure 5.13: Faulhaber MCDC 2803 Motion Controller - Functional Block Diagram

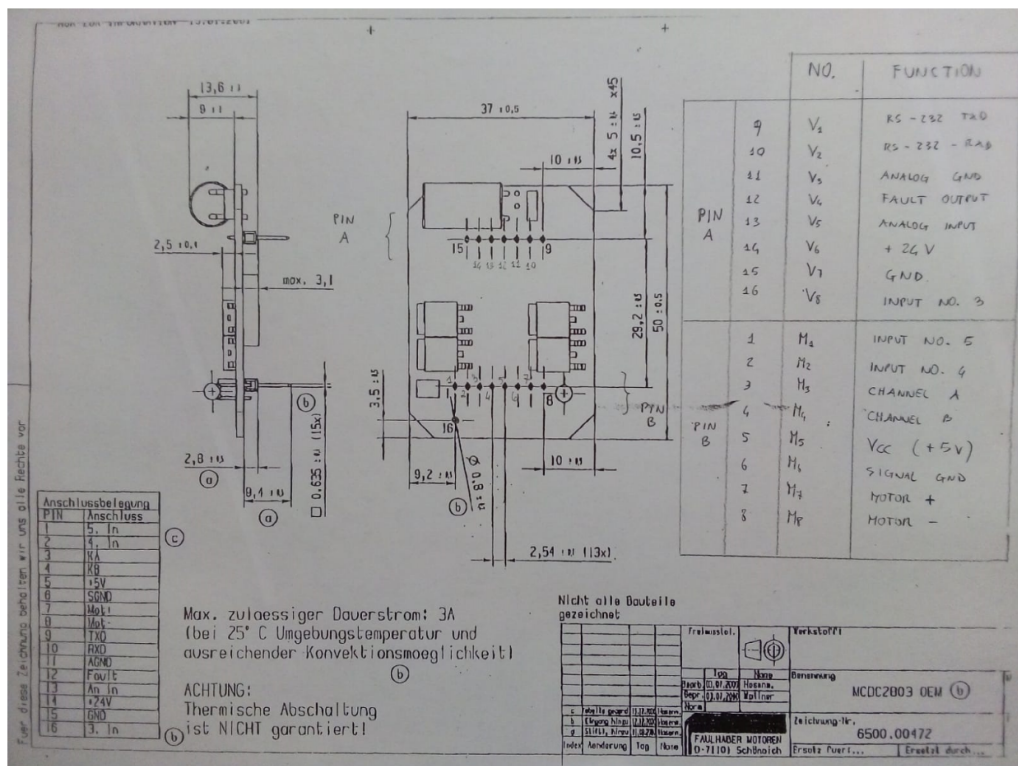


Figure 5.14: Faulhaber MCDC 2803 Motion Controller - Pinout

The motion controller was assembled with the electrical connections. These are the connection to gearmotor, to the supply power and to the serial communication port. The system is normally commanded via serial communication. However, it was predisposed a non-inverting amplifier if one wants to control the system in velocity, via a potentiometer and a low power signal. The gain of this amplifier is 2.

In figure 5.16 it is possible to see a dimensioning example of a non-inverting amplifier. The case considered is a 5V analogue voltage signal to be amplified until 10 V, because this is the analogue voltage signal to be provided to the motion controller.

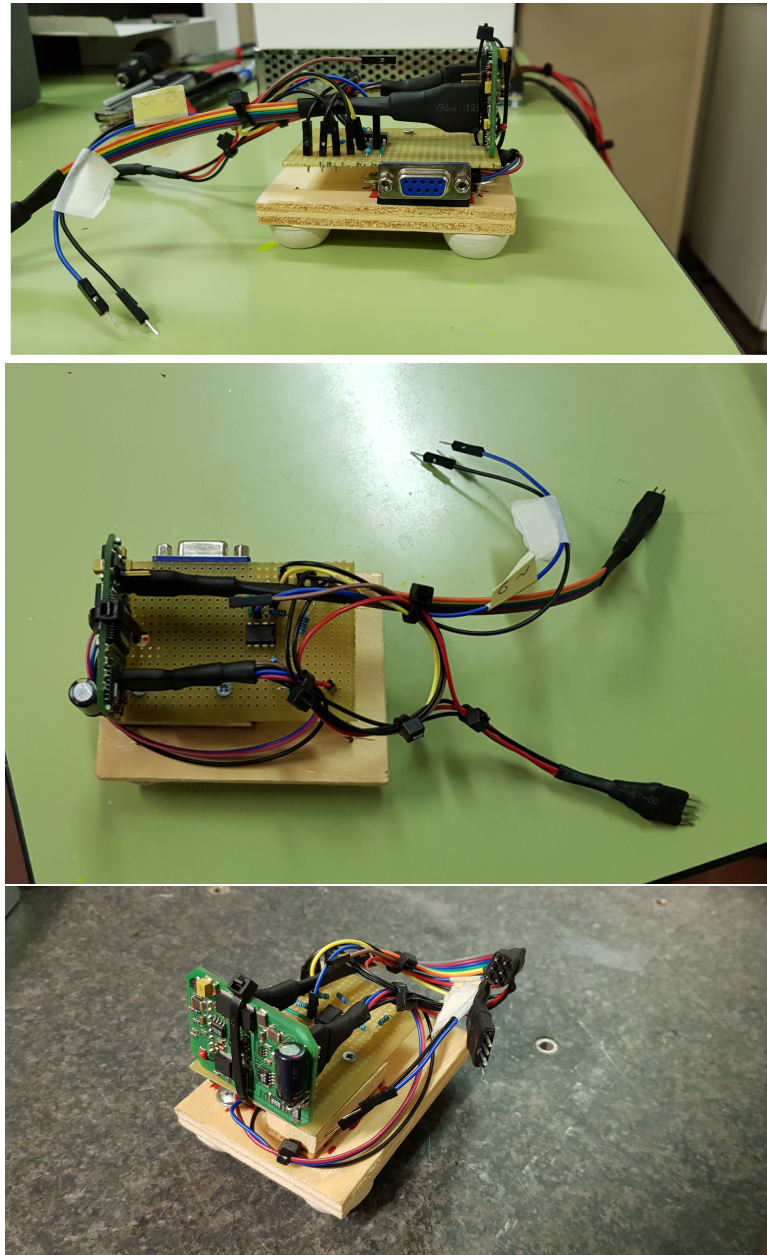


Figure 5.15: Motion Controller and related electronics

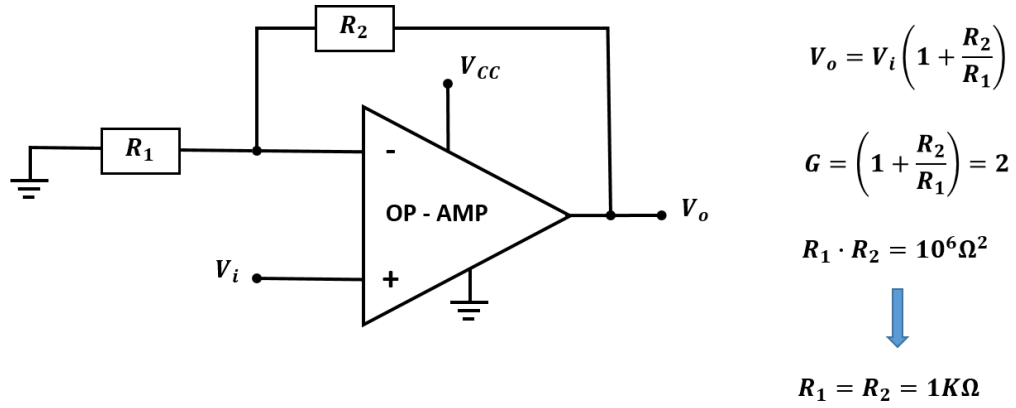


Figure 5.16: Non-inverting Amplifier with a gain $G = 2$ - Dimensioning

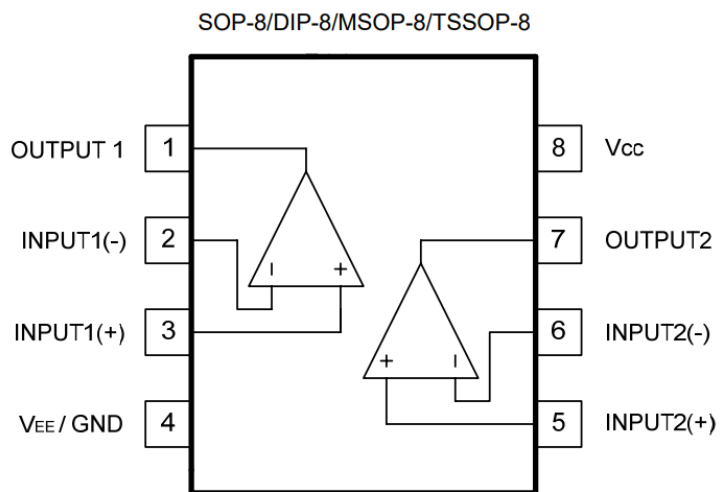


Figure 5.17: LM 358 Dual Operational Amplifier - Pinout

Power Supply

The power supply used is reported in figure 5.18. In table 5.7 are reported instead the power supply main characteristics.

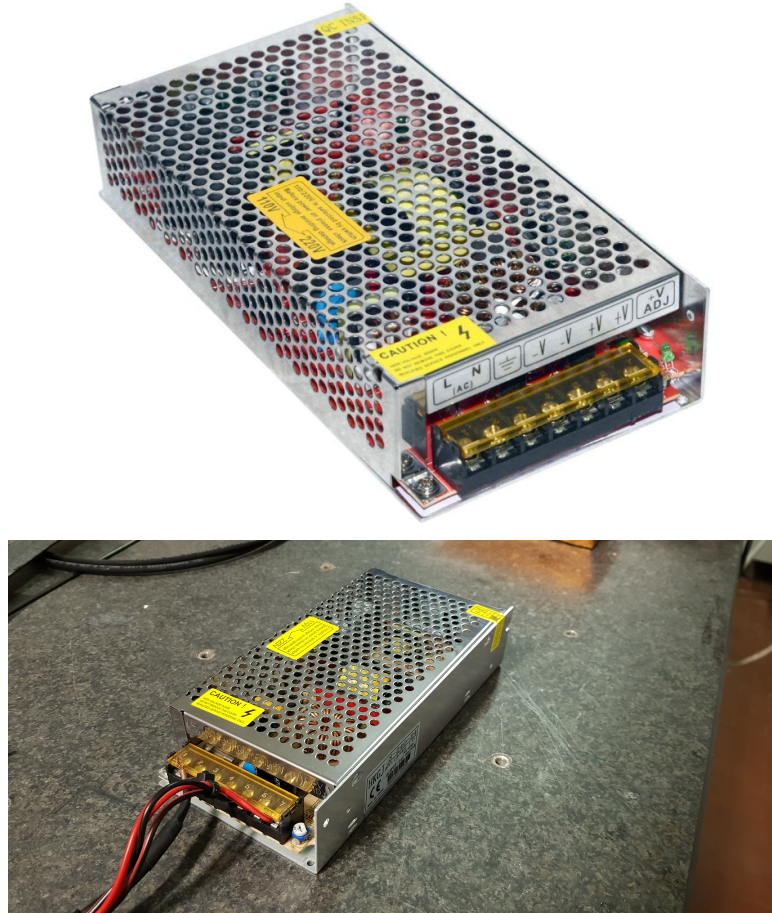


Figure 5.18: Supply Power

Parameter	Value
AC Input Voltage	110/220 V 1.1 V 50/60 Hz
DC Output Voltage	24 V
Output Current	10 A
Power	240 W

Table 5.7: Power Supply Main Characteristics

Functional Block Diagram

The working principle of this system is the same as the one reported in the Appendix A. The main difference are the components used for the scope. This is a less integrated system because it is assembled with some component that were available in the laboratory, like the gearmotor and the motion controller; some component were made, like the 3D printed supports and the aluminium adaptor; the rest of the components were bought.

In figure 5.19 it is possible to see the functional block diagram of the system. Meanwhile, in the figure 5.20 it is possible to see the response of the system in terms of Bragg wavelength of the optical fiber with the imposed tip displacement.

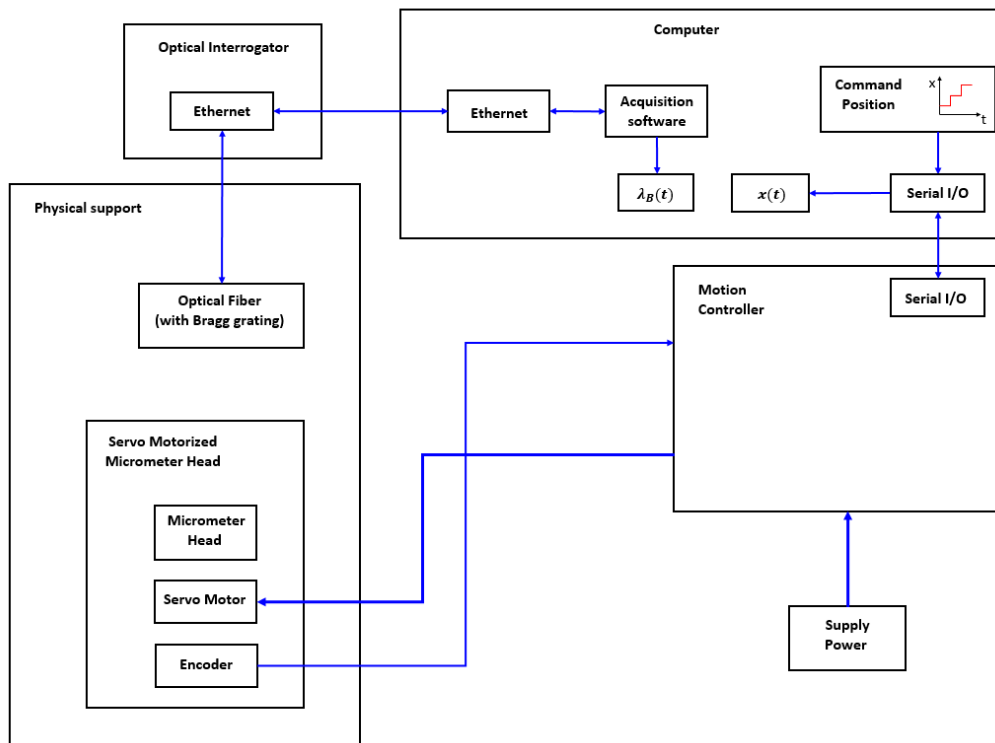


Figure 5.19: Spar Bending System Functional Block Diagram

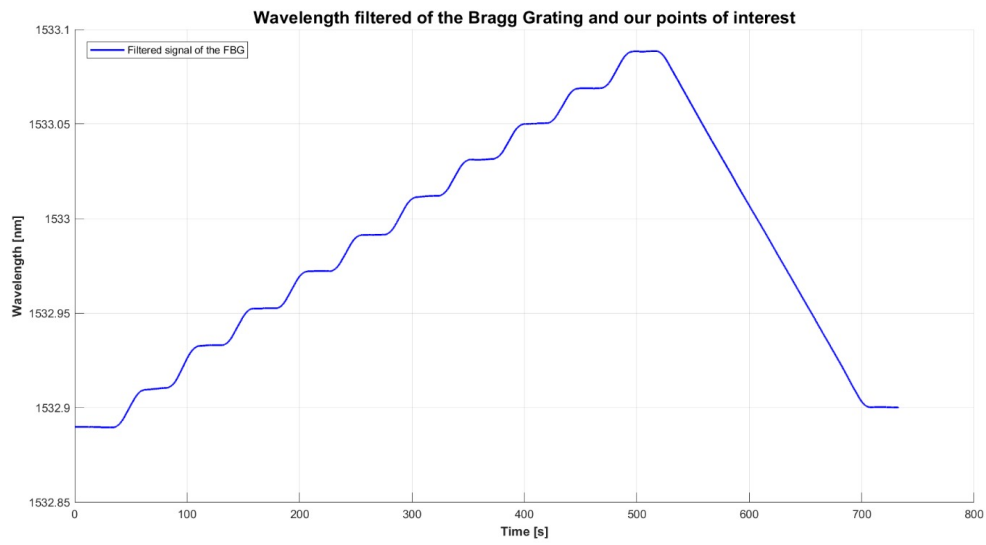


Figure 5.20: Response of the Optical Fiber with a 10 step command signal of 2 mm of tip displacement for each step

Bibliography

- [1] D. Ahuja, D. Parande, *Optical Sensors and their Applications*. November 2012, Journal of Scientific Research and Reviews Vol. 1(5).
- [2] Giurgiutiu, Victor, Fiber-Optic Sensors. *Structural Health Monitoring of Aerospace Composites*. s.l. : Academic Press, 2016.
- [3] Mihailov, Stephen J, *Fiber Bragg Grating Sensors for Harsh Environments*. February 2012.
- [4] Kersey, Alan D, Optical Fiber Technology. *A Review of Recent Developments in Fiber Optic Sensor Technology*. February 1996.
- [5] B. E. Saleh, M. C. Teich, *Fundamentals of Photonics, Second Edition* John Wiley and Sons, 2007.